



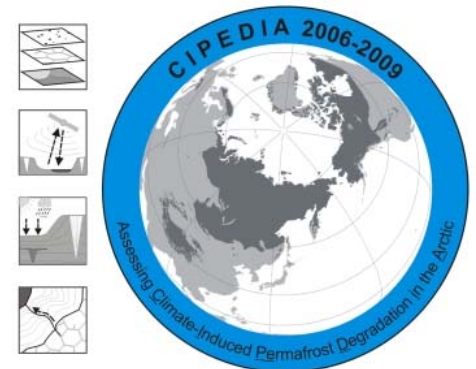
Remote Sensing of Changing Permafrost Landscapes in North Siberia

Projects and Some Results

Guido Grosse

Geophysical Institute, University of Alaska Fairbanks

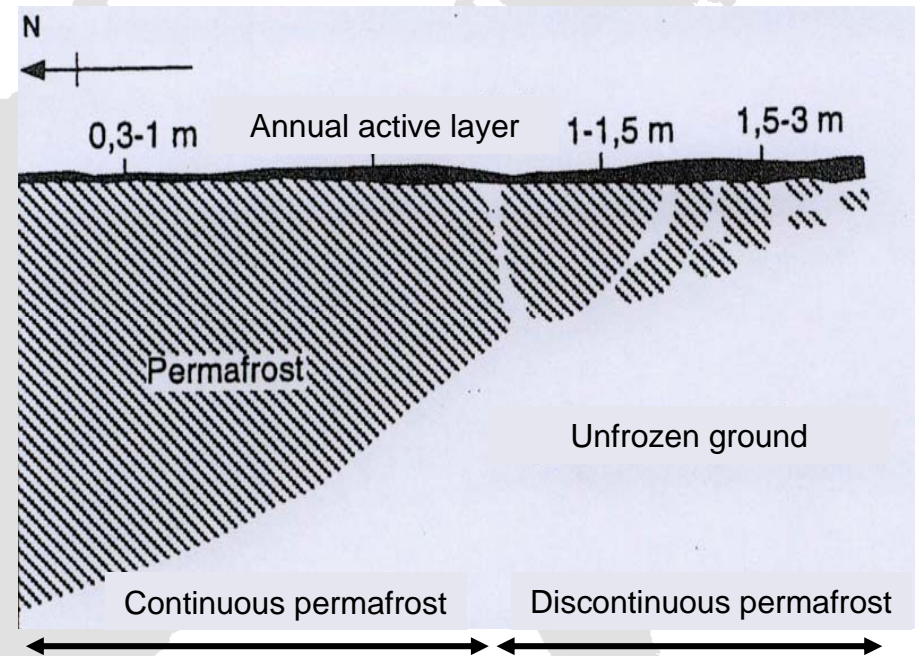
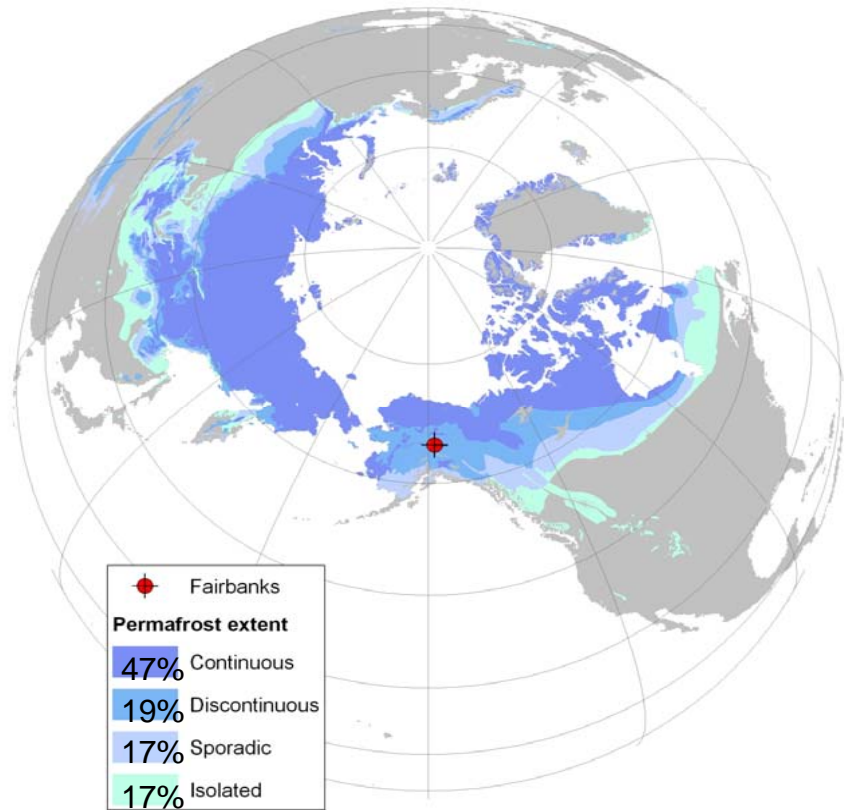
ASF Seminar – Nov 7, 2007



Permafrost definition and distribution

Permafrost is any ground that remains below or at 0°C for at least two consecutive years.

24% of the northern hemisphere land surface are affected by permafrost (Zhang et al. 1999).



Permafrost is an important factor for ecosystems, energy and matter cycles, infrastructure.

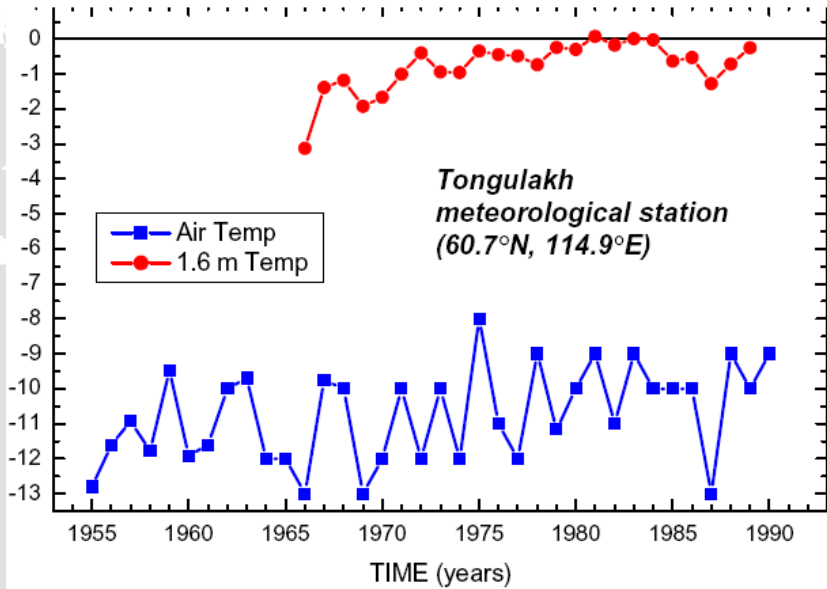
Permafrost degradation processes, time scales, and impacts are poorly known.

Thermal State of Permafrost (TSP)

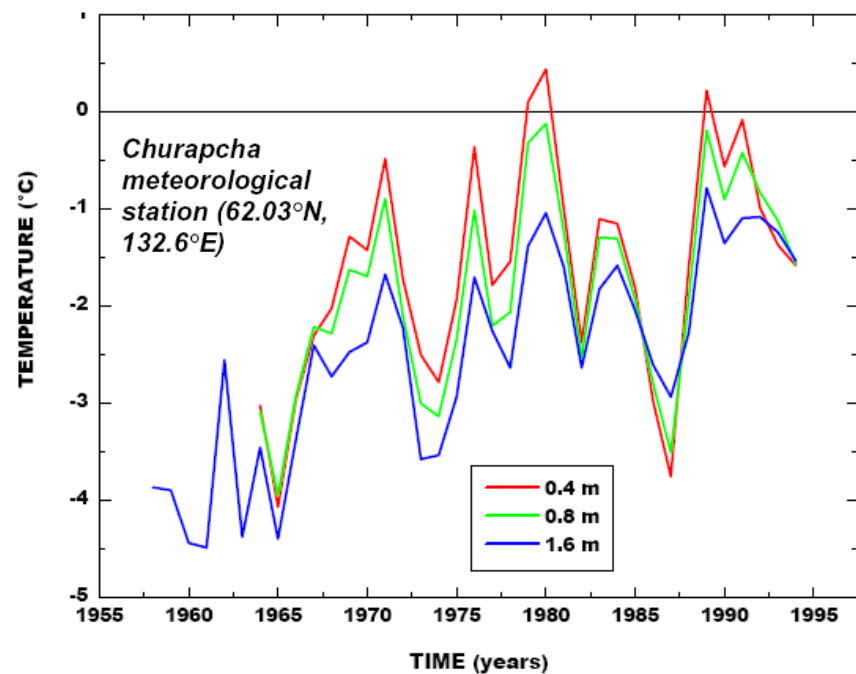
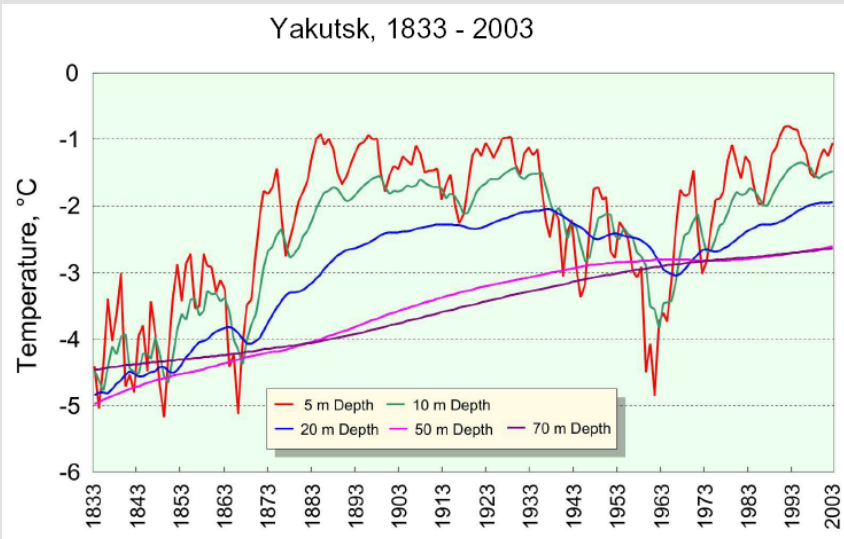


Romanovsky et al.

- International IPY endorsed project
- Funded by NSF (V. Romanovsky)
- Aiming at obtaining standardized ground temperature measurements in all permafrost regions
- Equipment of several 100 new boreholes in the circum-arctic with temperature data loggers
- Re-measurement of historic sites
- Contemporary snapshot of the thermal state of the permafrost realm
- Delivers data for modelling future trajectory of permafrost



Contemporary changes in central Yakutia



Definition of ,permafrost degradation‘

- A naturally or artificially caused decrease in the thickness and/or areal extent of permafrost (National Research Council of Canada Technical Memorandum No.142.1988).

Expressed as

- a thickening of the active layer
- a lowering of the permafrost table
- a reduction in the areal extent
- or the complete disappearance of permafrost.

In the Russian literature the term degradation usually is more specific in that permafrost starts to degrade when winter freezing no longer reaches the permafrost table and taliks begin to form. The formal indicator of this event is the mean annual temperature at the bottom of the active layer (seasonally frozen or seasonally thawed). Permafrost degradation begins when this temperature remains persistently above 0°C.

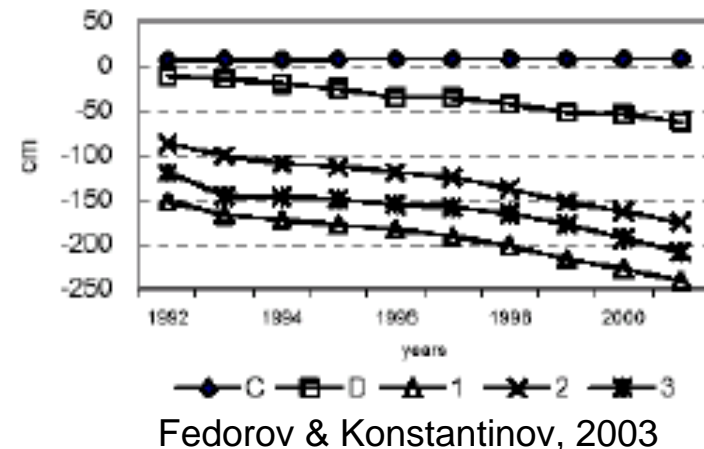
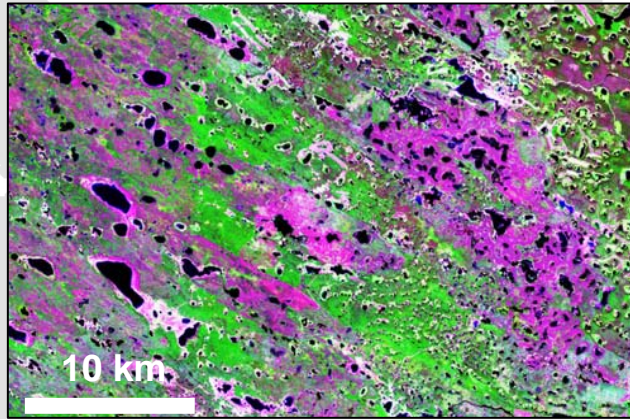
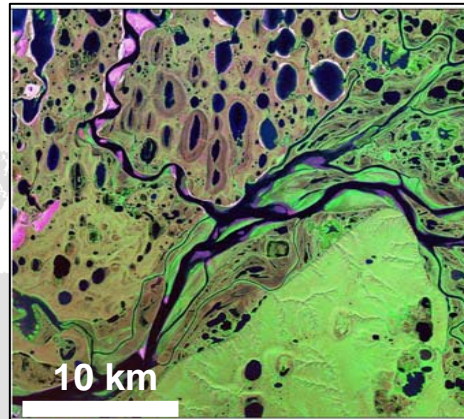


Figure 3. Surface subsidence in thermokarst depression, site 2. C – check point, undisturbed inter-alaras area; D – incipient thaw depression; 1-3 – centers of polygons within thaw depression.

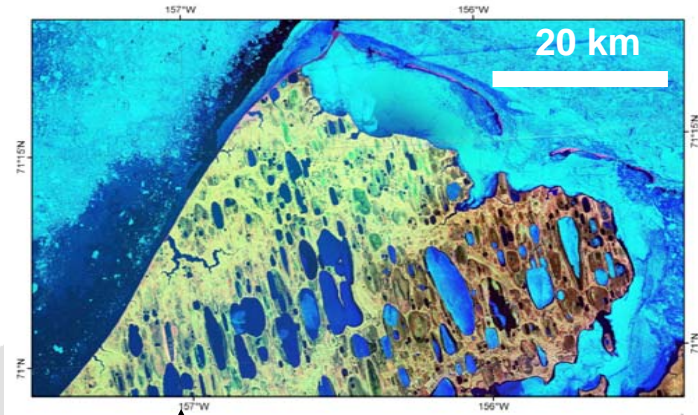
Thermokarst: Processes and landforms resulting from the thawing of ice-rich ground, i.e. the surface subsidence related to the volume loss due to ground ice melting.



Yakutsk, Central Siberia



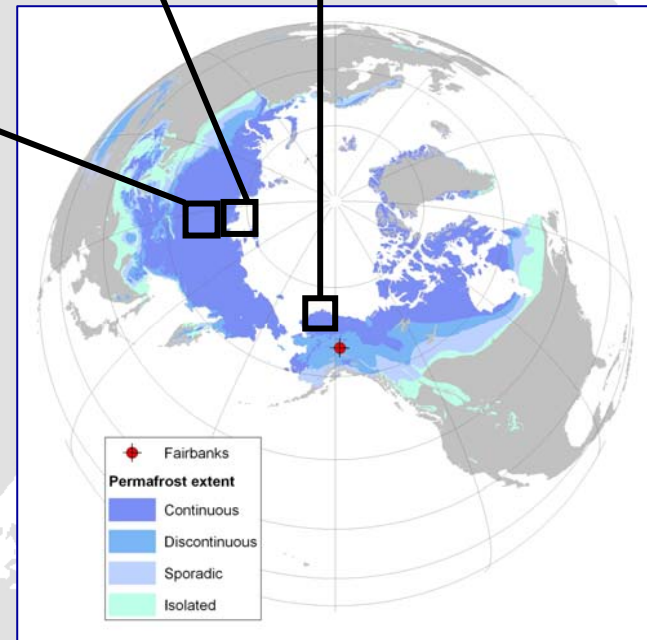
Lena Delta, North Siberia



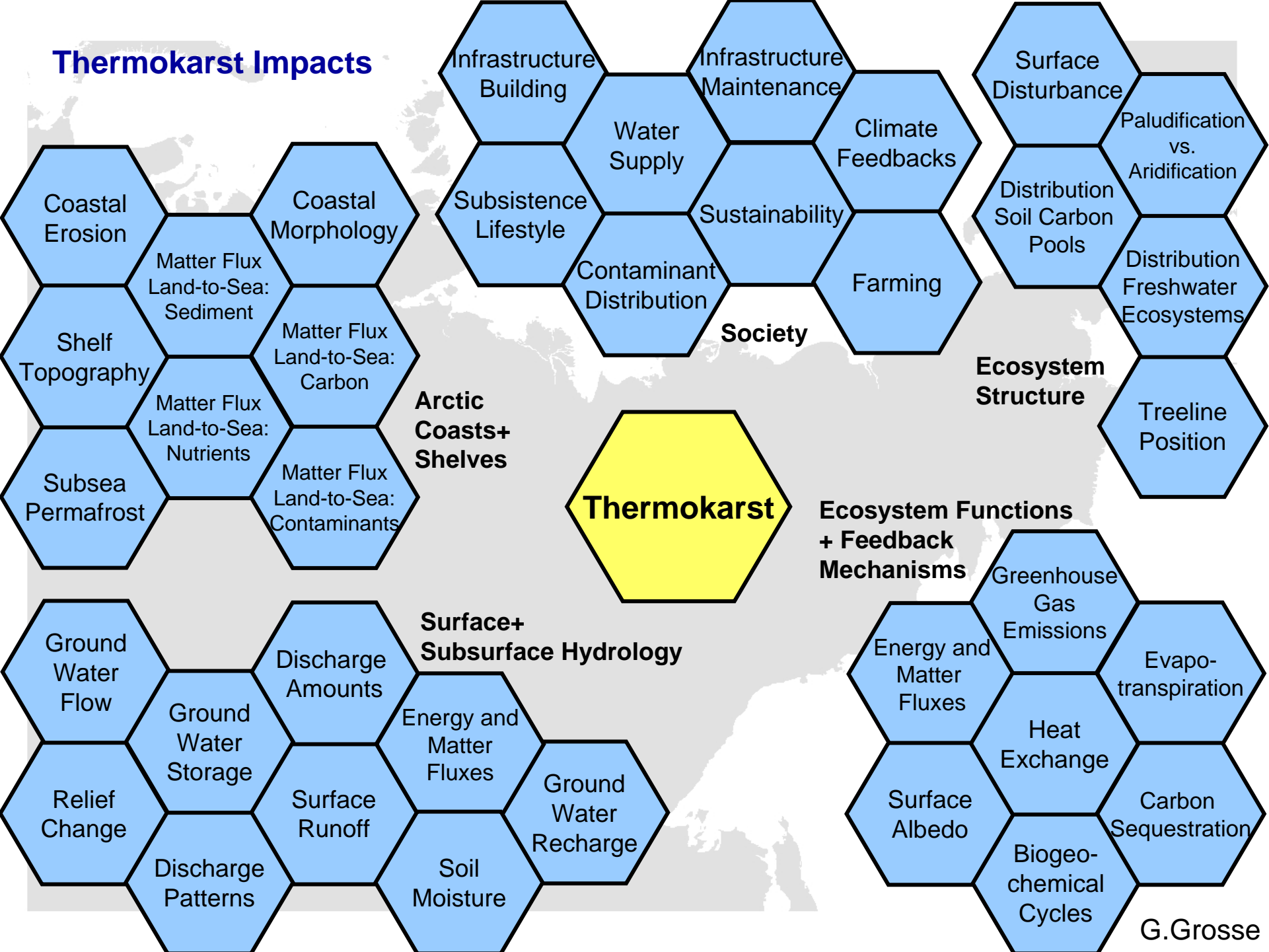
Barrow, North Alaska

Two Main Messages:

- *Permafrost degradation is not restricted to the southern permafrost boundary, where warm permafrost prevails*
- *Permafrost degradation is closely related to topographical + hydrological change*

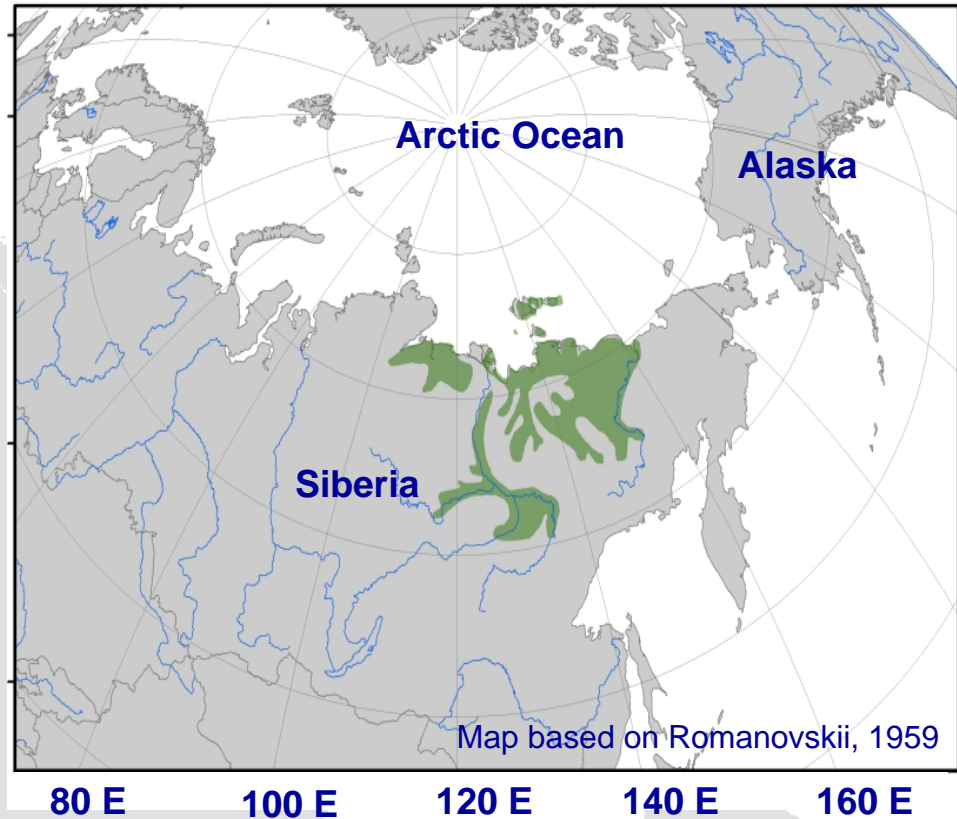


Thermokarst Impacts



Thermokarst

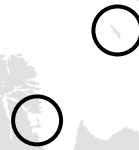
Distribution of Ice-Rich Permafrost (Yedoma) in Northeast Siberia



- Thickness of the deposit is between 5-100m
- Present day total coverage is $> 1 \times 10^6$ km
- Gravimetric ground ice contents in the sediments between 60-120%
- Including the ice wedges, total volumetric ice content of up to $> 75\%$
- Organic carbon content averages between 2-5%
- Accumulation during several 10 000 years

Ice-rich Permafrost Enhances Coastal Erosion

In NE Siberia, steep cliffs consisting of ice-rich permafrost can be up to 40m high



Bykovsky Peninsula, Laptev Sea



Stolbovoy Island, Laptev Sea

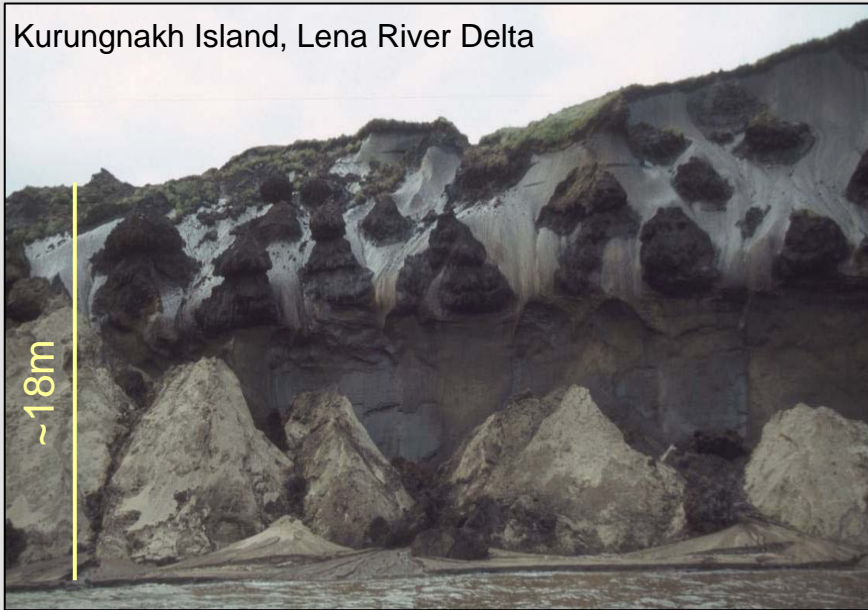


Ice-rich Permafrost Enhances Coastal Erosion

Coastal erosion rates in the NE Siberian Seas can reach up to 12m/year



Kurungnakh Island, Lena River Delta



Oyagoss Yar coast, East Siberian Sea



Ice-rich Permafrost Enhances Coastal Erosion

At some sites, coastal erosion resulted in up to several 100m of coastal retreat during the remote sensing period (~60 years)



Mamontov Klyk, Laptev Sea

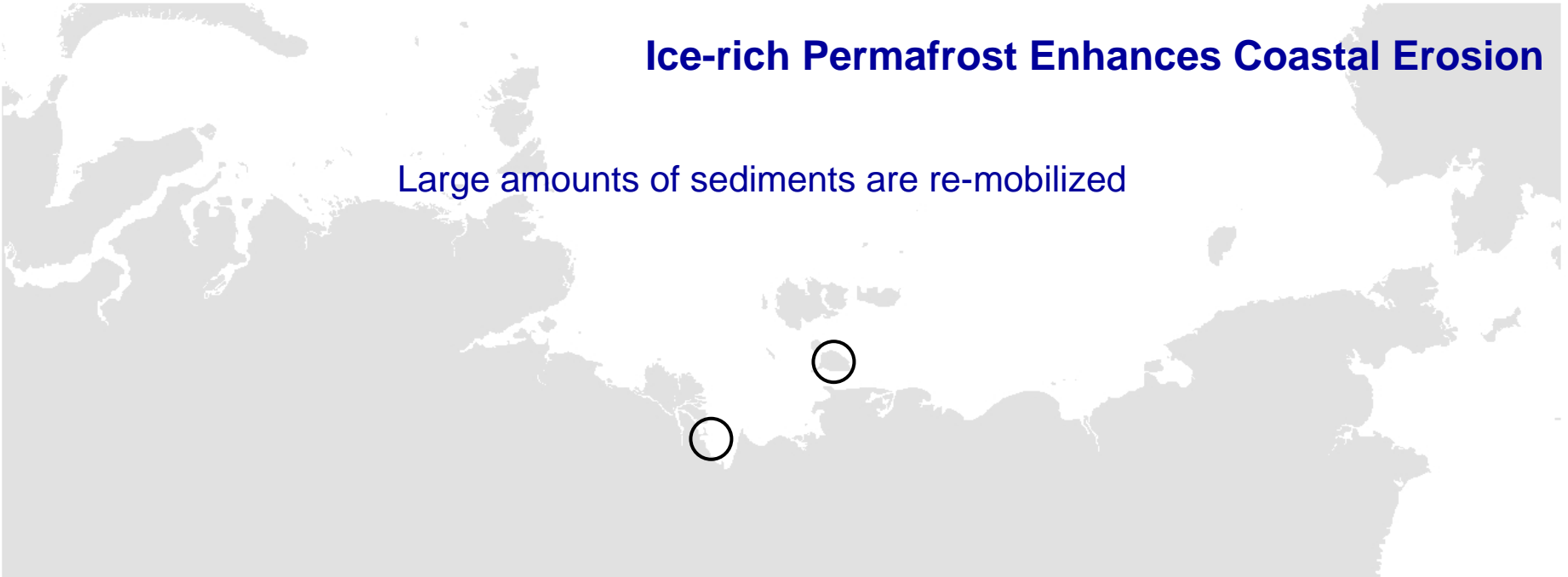


Duvanny Yar, Kolyma Lowland



Ice-rich Permafrost Enhances Coastal Erosion

Large amounts of sediments are re-mobilized



Muostakh Island, Laptev Sea



Bolshoy Lyakhovskiy Island, Laptev Sea



Permafrost Degradation and C-Cycle

Organic carbon that was stored for several ten thousands of years is released by coastal erosion, thermo-erosion, and thermokarst into the active carbon cycle

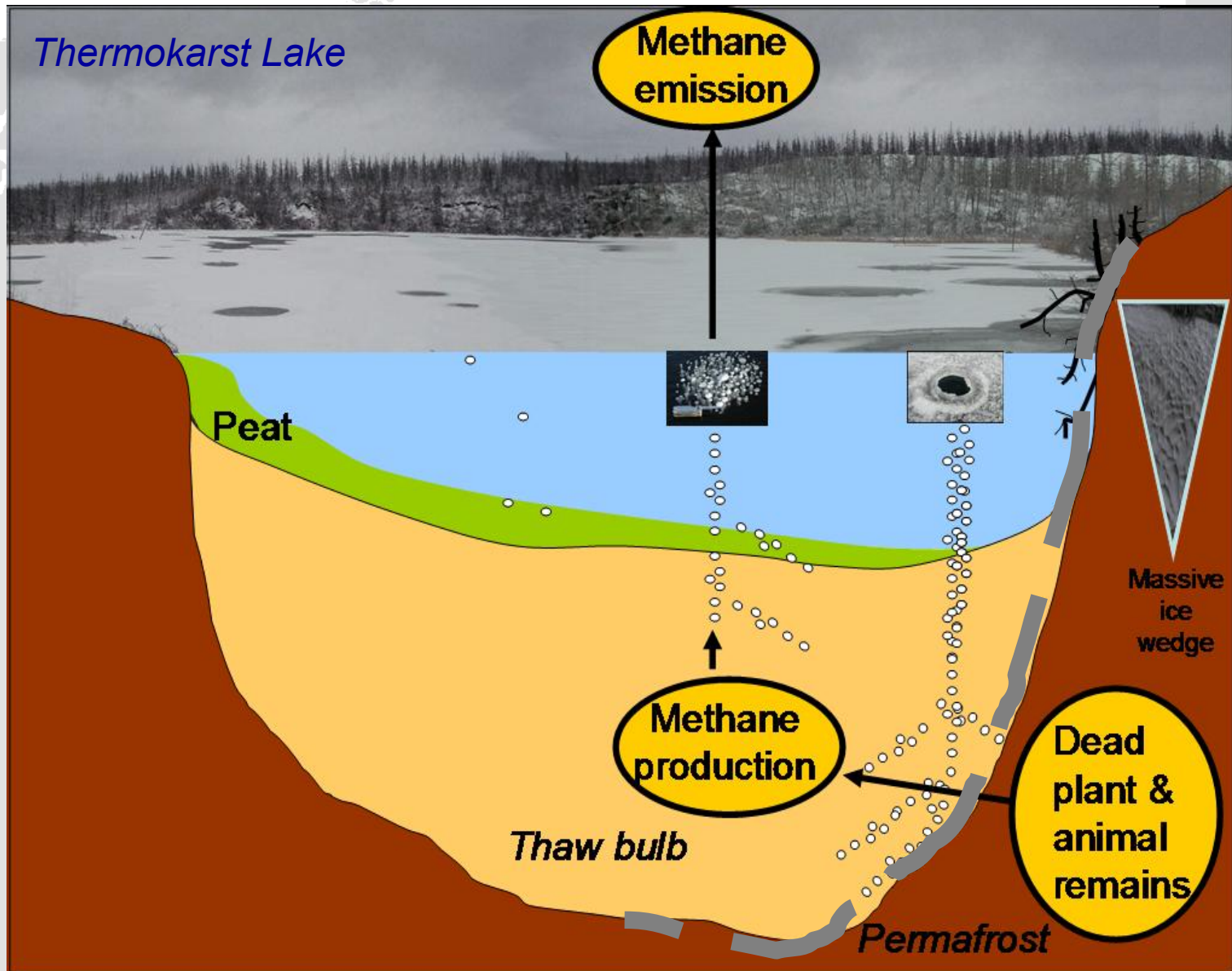
Thermo-erosion of organic-rich, frozen deposits



Coastal erosion of organic-rich, frozen deposits

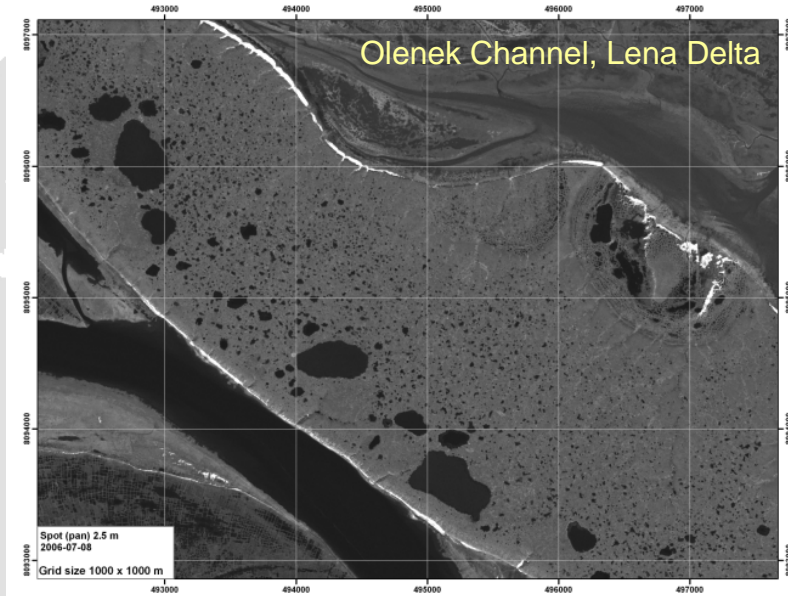


Permafrost Degradation and C-Cycle



Permafrost Degradation and C-Cycle

Methane emission from thermokarst lakes due to anaerobic degradation of released organic material



Tools and techniques for assessing permafrost degradation

Multi-temporal field monitoring on selected sites

- Surface and subsurface climate station data
- Mapping and change detection (active layer depth, subsurface temperatures, vegetation, soil moisture, surface subsidence, hydrology)
- Temporal patterns: Geochronology of permafrost degradation

Multi-temporal and multi-sensoral remote sensing

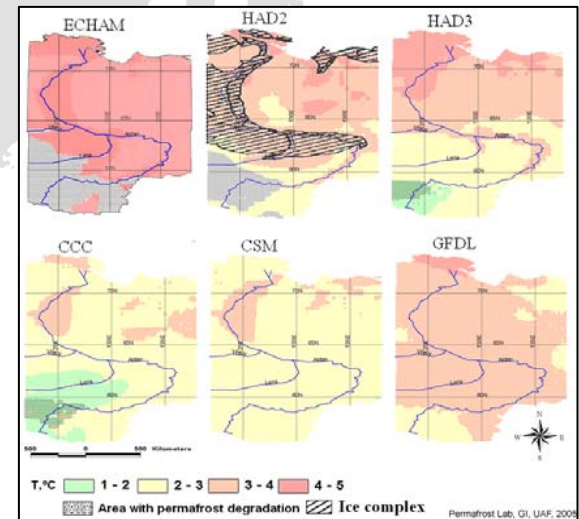
- Mapping and monitoring of permafrost degradation features (high spatial resolution)
- Provision of physical input parameters for modeling (various spatial and spectral resolutions)

GIS-based spatial analysis

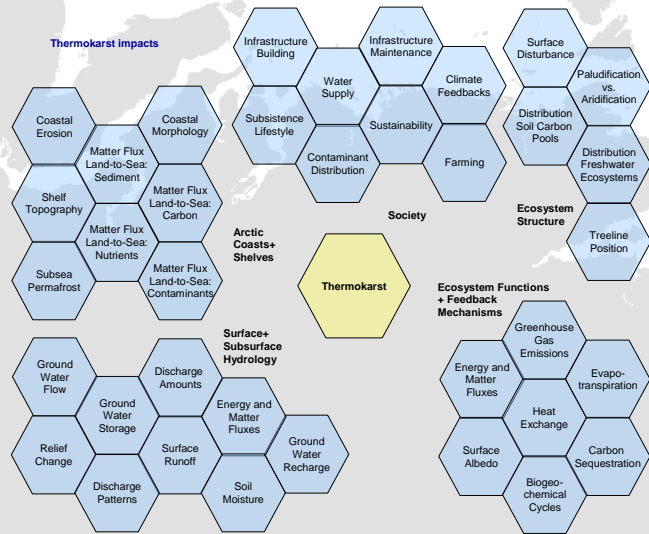
- Spatial distribution of permafrost degradation features
- Relationship with other features (permafrost types, ice contents, sediment thickness, climate, hydrology, soils, vegetation, etc.)
- Quantification of processes and feedbacks (e.g. carbon, sediment, and energy fluxes; interactions with vegetation, hydrology, and coasts)

Retrospective and prognostic modeling

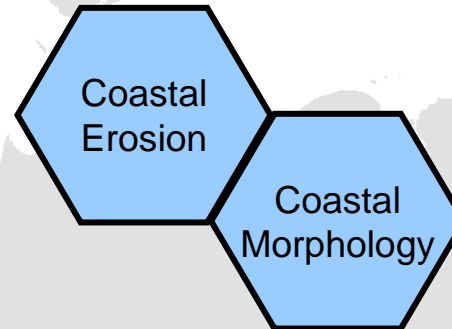
- Permafrost models
- Climate models
- Coupled models



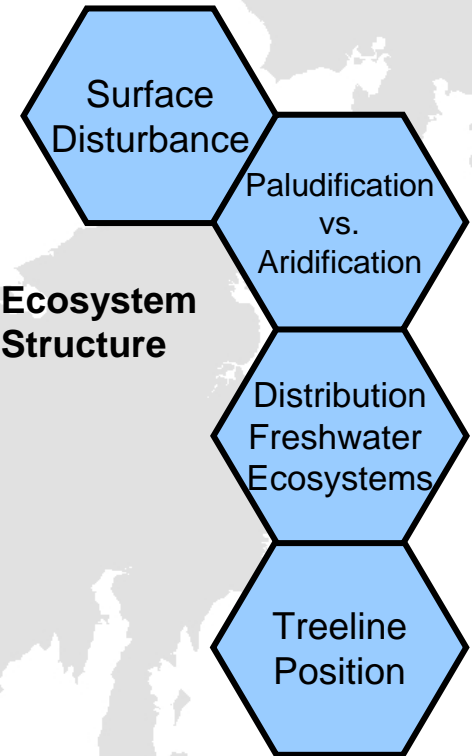
Key parameters that can be measured with remote sensing sensors



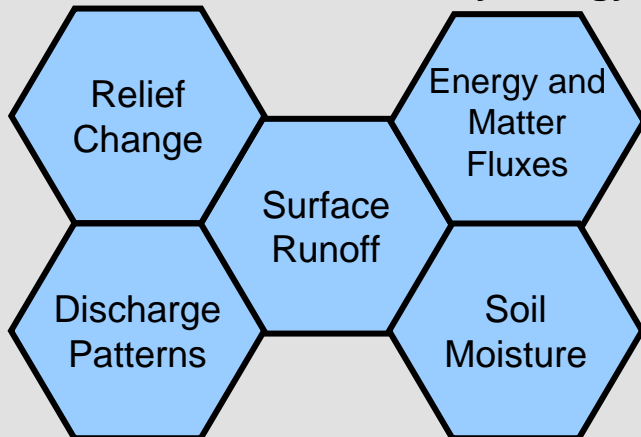
Arctic Coasts + Shelves



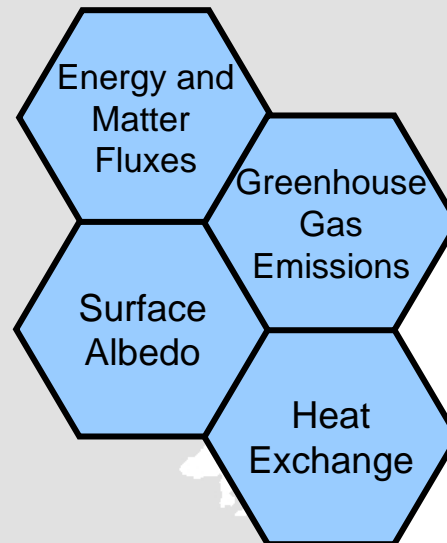
Ecosystem Structure



Surface + Subsurface Hydrology



Ecosystem Functions + Feedback Mechanisms





**Projects focusing on the survey of a status baseline or changes in the system
with a remote sensing component**

G. Grosse: Climate-Induced Permafrost Degradation in the Arctic (CIPEDIA)

K. Walter: Impacts of Thermokarst Lakes on Carbon Cycling and Climate Change

V. Romanovsky: Permafrost Dynamics Within the Northern Eurasian Region and Related Impacts on Surface and Sub-Surface Hydrology

P. Overduin: Arctic Circum-Polar Coastal Observatory Network (ACCO-Net)

+ many projects focusing on local studies, e.g.:

Coastal Erosion at the Bykovsky Peninsula

Morphometry and Spatial Distribution of Lakes in the Lena River Delta

Methane Balance of the Wetlands in the Lena River Delta

Spectral Properties of Periglacial Landscapes in the Lena River Delta

Overview of remote sensing data used or planned for use in these studies

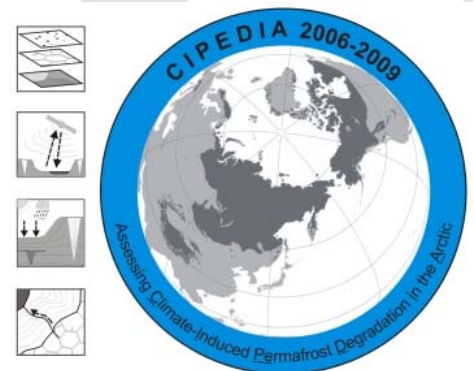
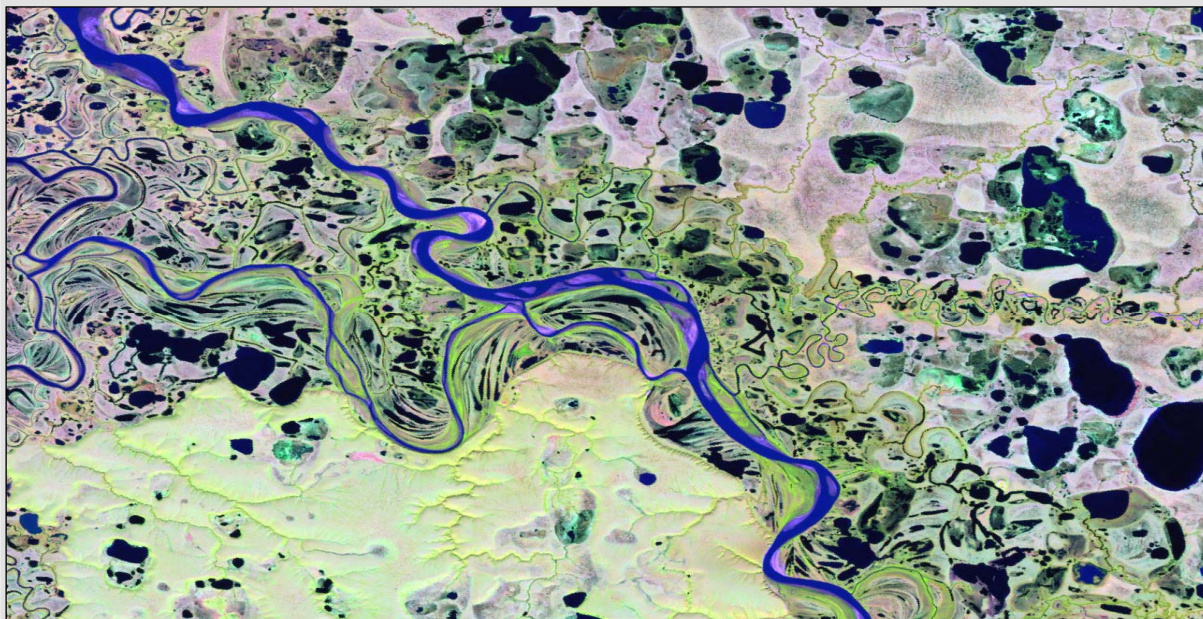
	<i>Bands</i>	<i>Wavelength</i>	<i>Ground resolution</i>	<i>Period of operation</i>	<i>Currently used or planned for use in these studies</i>
<i>Aerial imagery</i>	1	<i>Pan</i>	0.8 – 2m	ca. 1951-	<i>Coastal erosion, lake change, thermokarst distribution</i>
<i>Corona KH-1 to 4B</i>	1	<i>Pan</i>	up to 1.8m	1959-1972	<i>Coastal erosion, lake change, thermokarst distribution</i>
<i>Gambit KH-7</i>	1	<i>Pan</i>	up to 0.6m	1963-1967	
<i>Ikonos-2</i>	5	<i>VIS-VNIR, pan</i>	4.0 / 1.0m	1999-	<i>Lake change</i>
<i>Landsat-7 ETM+</i>	8	<i>VIS-SWIR, TIR, pan</i>	30 / 60 / 15m	1999-	<i>Thermokarst distribution</i>
<i>Terra MODIS</i>	36	<i>VIS-SWIR, TIR</i>	250-1000m	1999-	<i>Land surface temperatures</i>
<i>CHRIS Proba</i>	18	<i>VIS-VNIR</i>	17m	2001-	<i>Thermokarst distribution, spectral characteristics</i>
<i>Spot-5</i>	5	<i>VIS-VNIR, pan</i>	10 / 2.5m	2002-	<i>Coastal erosion, lake change</i>
<i>ALOS PRISM</i>	1	<i>Pan</i>	2.5m	2006-	<i>Coastal erosion, lake change, Thermokarst distribution</i>
<i>ALOS AVNIR-2</i>	4	<i>VIS-VNIR</i>	10m	2006-	
<i>Radarsat</i>		<i>SAR</i>	10m	1995-	<i>Upscaling of methane emissions from lakes</i>
<i>ALOS PALSAR</i>		<i>SAR</i>	10m	2006-	<i>SAR interferometry</i>

Climate-Induced Permafrost Degradation in the Arctic

G. Grosse, V. Romanovsky

Objectives

- Baseline classification of the different types of permafrost degradation terrain
- Qualitative and quantitative assessment of thermokarst distribution
- Based on multi-sensoral remote sensing, field data, and spatial data analysis

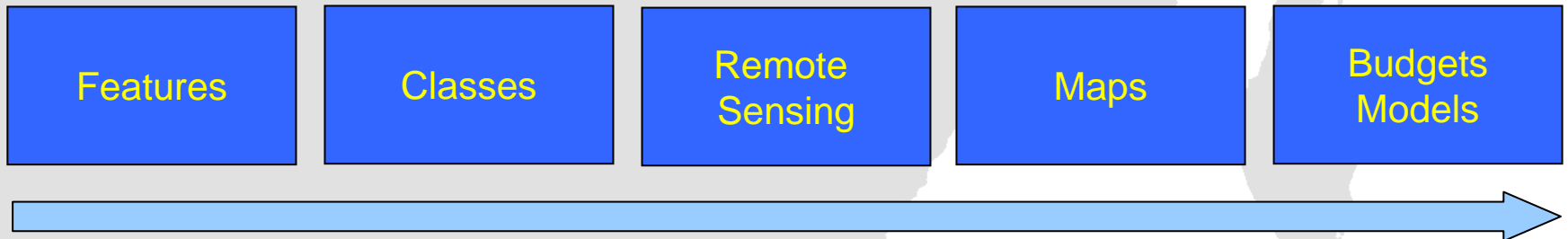


Climate-Induced Permafrost Degradation in the Arctic

G. Grosse, V. Romanovsky

Important Steps for a Circum-Arctic Classification and Assessment

- *Identify surface and subsurface properties, features and structures indicative for permafrost degradation*
- *Define a valid, unified and widely accepted classification scheme for permafrost degradation*
- *Develop and apply methods to detect (RS), quantify (GIS) and predict (Models) permafrost degradation*



Climate-Induced Permafrost Degradation in the Arctic

Within an upcoming (2008-2010) NSF IPY project (Walter & Grosse et al.: Understanding the impacts of thermokarst lakes on C cycling and climate change), the following tasks are proposed:

Create a medium resolution circum-arctic map of ice-rich yedoma deposits (largely Siberia + Alaska)

- *Based on geological and geocryological field data and maps, RS imagery, and DEM*

Map the distribution of thermokarst lakes and alases in regions with yedoma and yedoma-like deposits

- *From key sites to the entire yedoma region: Upscaling*
 - *Thermokarst lake detection and classification*
 - *Alas detection and classification (based on geomorphology, spectral+textural properties, and DEM)*
 - *Define scaling rules for extrapolating thermokarst classifications from local to regional datasets*
-

Monitor the recent dynamics of thermokarst lakes and basins at the study sites

- *Quantify the changes by thermokarst lake expansion using high-resolution RS data, ca. 1950-2010*
- *Ground truth with high-accuracy kinematic differential GPS (D-GPS) surveys along the lake shores*
- *Spectral surface characterization with a portable field spectrometer (ASD Fieldspec Pro FR) of areas with known thermokarst disturbance, for comparison with undisturbed sites, and for the identification of disturbed areas in multi-spectral RS images*

Permafrost Dynamics Within the Northern Eurasian Region and Related Impacts on Surface and Sub-Surface Hydrology

V. Romanovsky, S. Marchenko & C. Duguay

Objectives

- Obtain a deeper understanding of the temporal (interannual to centennial time scales) and spatial (north to south and west to east) variability and trends in the active layer characteristics and permafrost temperatures in the 20th century and their impact on hydrology within the Northern Eurasia region*
- Develop more reliable predictive capabilities for the projection of these changes into the 21st century*

Data Acquisition

*Landscape characteristics
Meteorology
Active layer
Permafrost temperatures
GIS
Hydrogeology*

Remote Sensing

*Identify relevant products
Acquire base data
Use as physical model
parameter*

Modeling

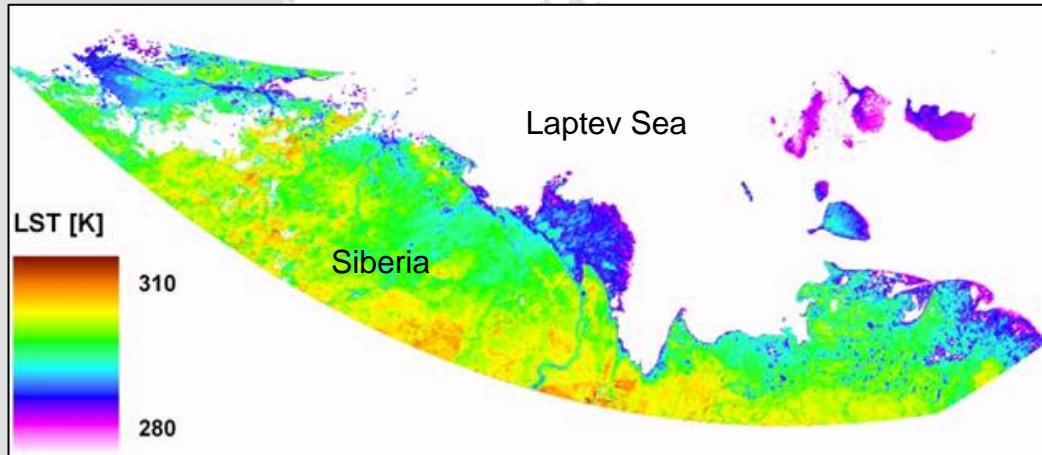
*Calibrate models at key sites
Reconstruct past temperature regimes
Improve existing model
Forecast future temperature regime*

Permafrost Dynamics Within the Northern Eurasian Region and Related Impacts on Surface and Sub-Surface Hydrology

V. Romanovsky, S. Marchenko & C. Duguay

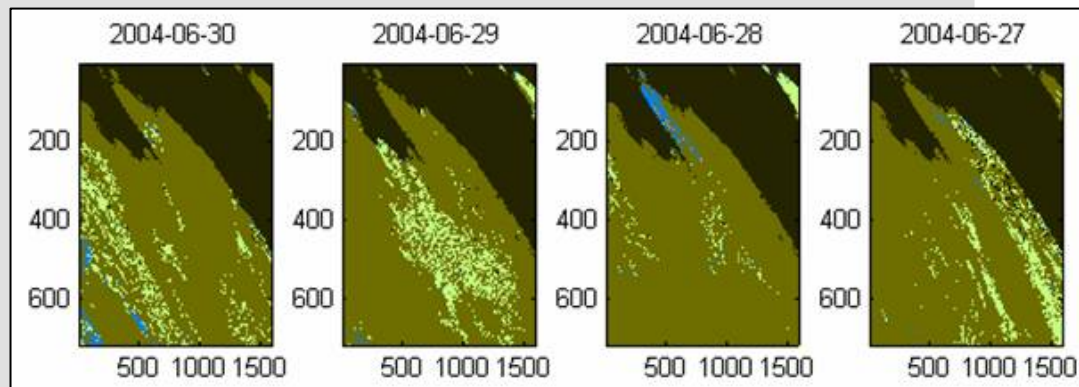
Remote Sensing

- e.g. Land Surface Temperatures (LST) derived from Terra + Aqua MODIS



LST for the Laptev Sea region from 2006-07-09

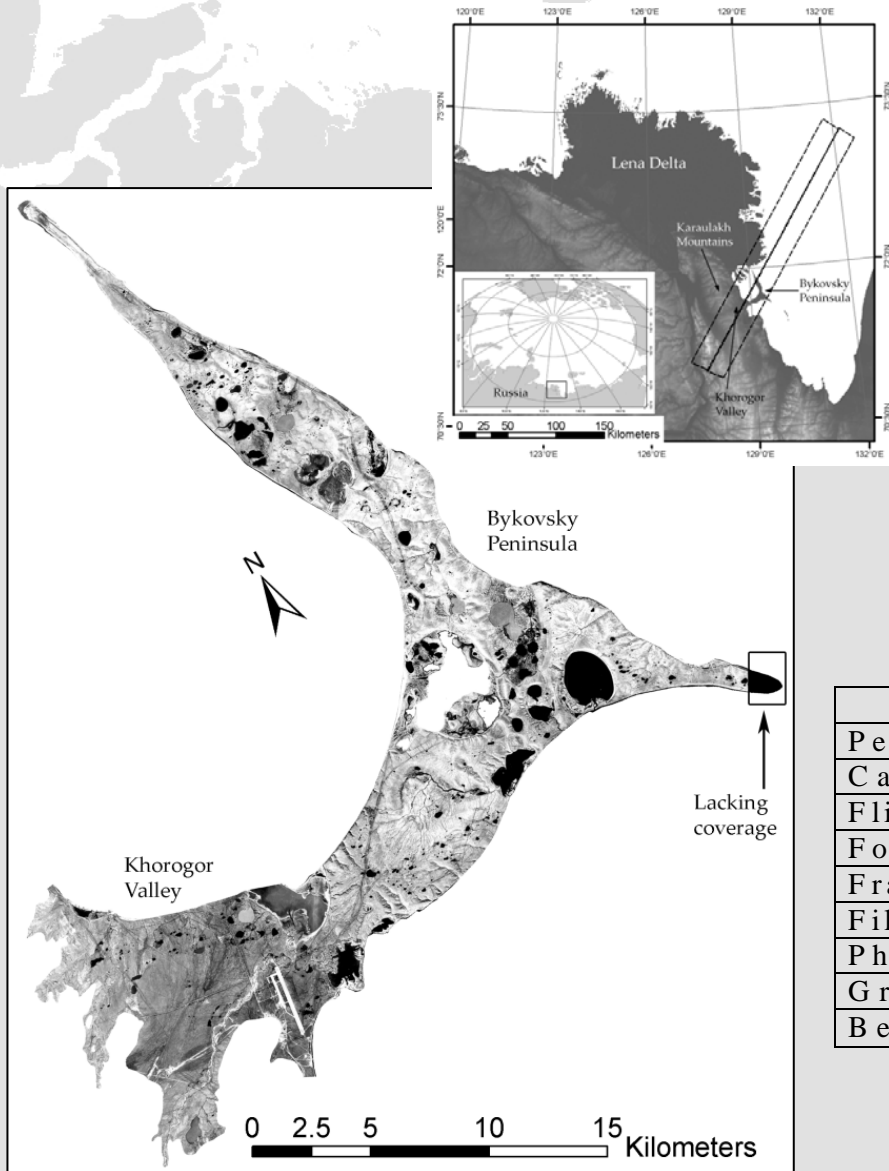
- e.g. snow cover derived from Terra + Aqua MODIS



Snow cover for the Lena River Delta derived from MOD10A1

Application of Historical Declassified Satellite Data for Periglacial Studies

G. Grosse, L. Schirrmeister, V. Kunitsky, H.-W. Hubberten



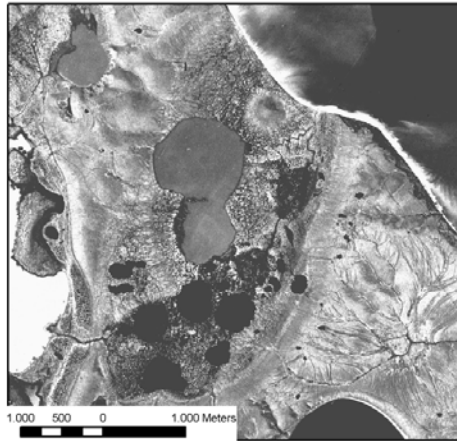
CORONA images used	D003003M1107-1AFT D003002M1107-1AFT
Date of acquisition	24 th July 1969
Film size per image subset	5.5 x 14 cm
Ground coverage per subset	13.8 x 35 km
Scan resolution	7 μ m (3600 dpi)
Ground resolution	2.5 m

Satellite KH-4B	
Period of operation	15/09/1967-25/05/1972
Camera type	J-3, panchromatic
Flight altitude	150 km
Focal length	61 cm
Frame format	5.5 cm x 75.7 cm
Film resolution	160 lines / mm
Photo scale of the film	1:247,500
Ground coverage	13.8 km x 188 km
Best ground resolution	1.8 m

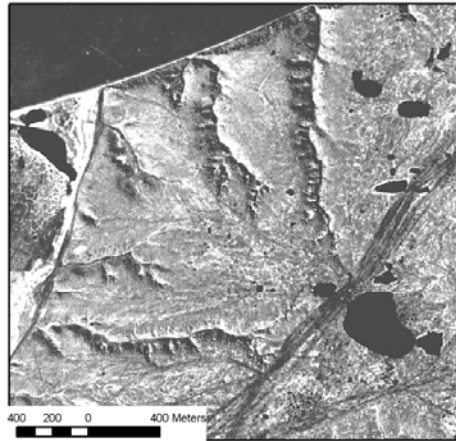
Application of Historical Declassified Satellite Data for Periglacial Studies

G. Grosse, L. Schirrmeyer, V. Kunitsky, H.-W. Hubberten

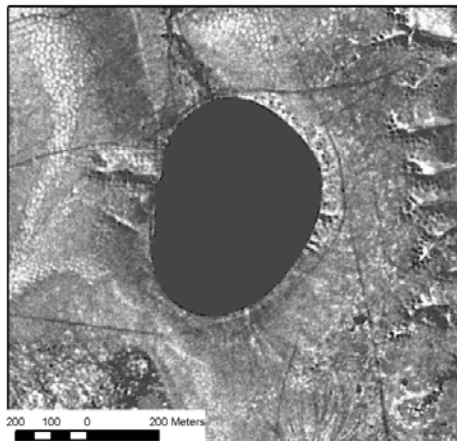
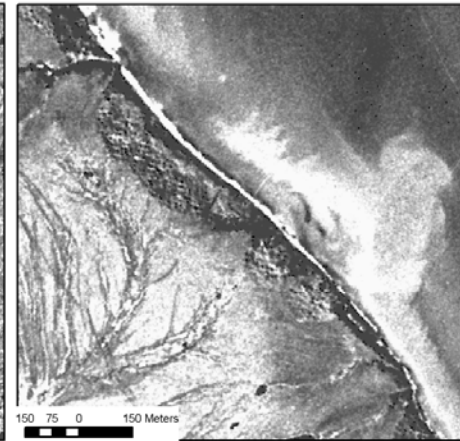
Thermokarst depression



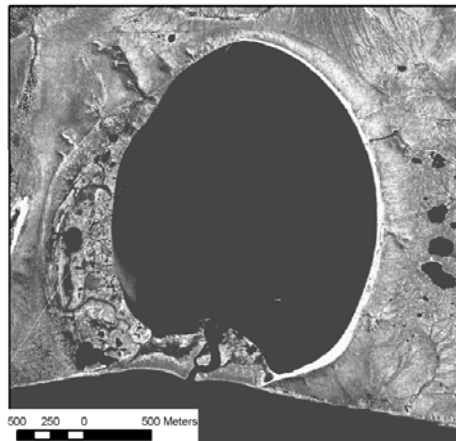
Thermo-erosional valleys



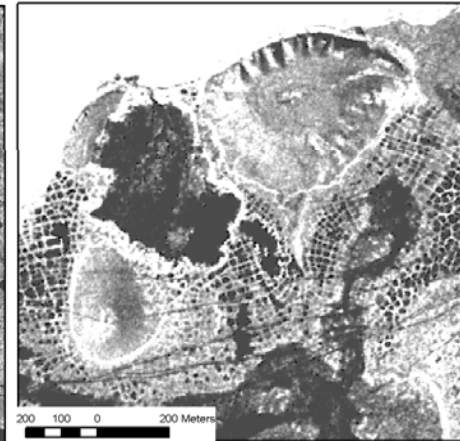
Retrogressive thaw slumps



Thermokarst lake



Thermokarst lagoon

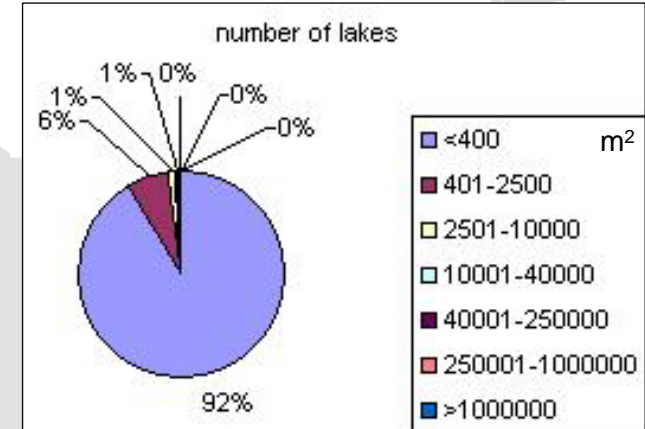
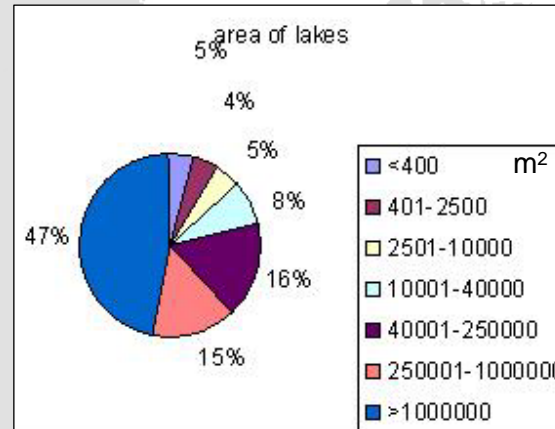
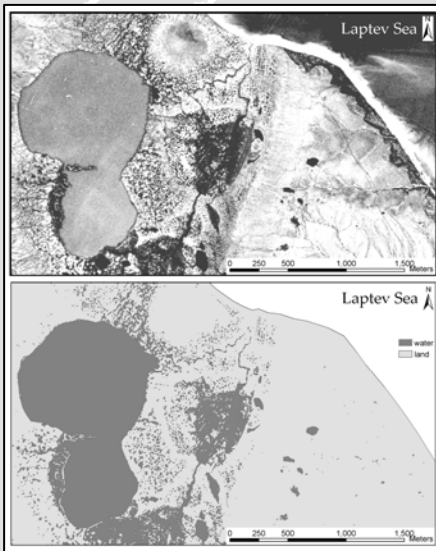


Pingos + ice wedge polygons

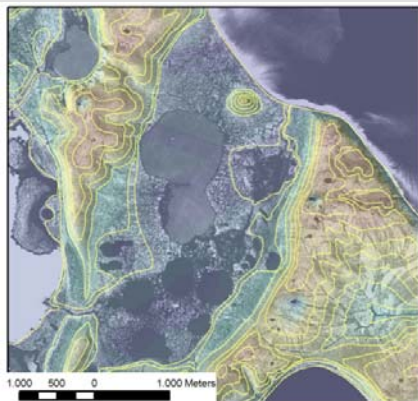
Application of Historical Declassified Satellite Data for Periglacial Studies

G. Grosse, L. Schirrmeister, V. Kunitsky, H.-W. Hubberten

- Mapping surface features (geomorphology, hydrology)
- Extending the temporal range of high-resolution lake change and coastal erosion studies in regions without accessible aerial imagery



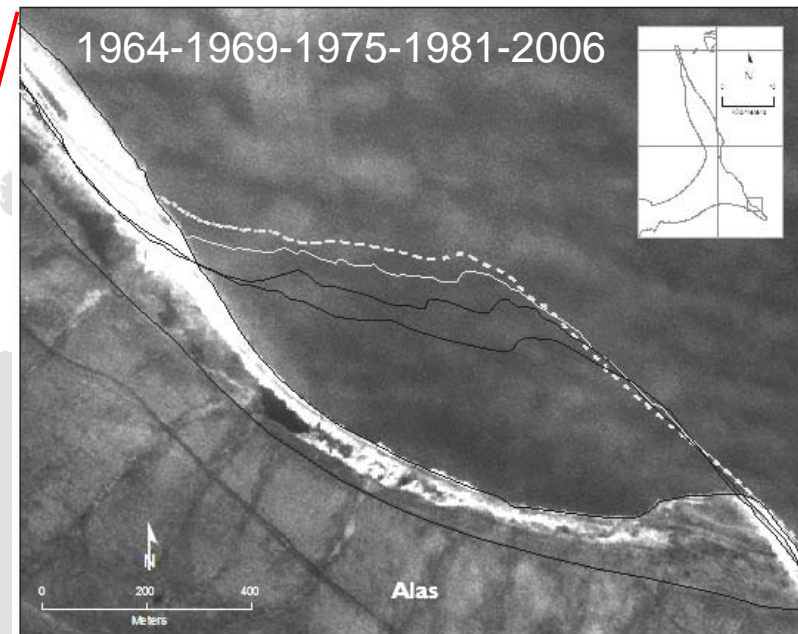
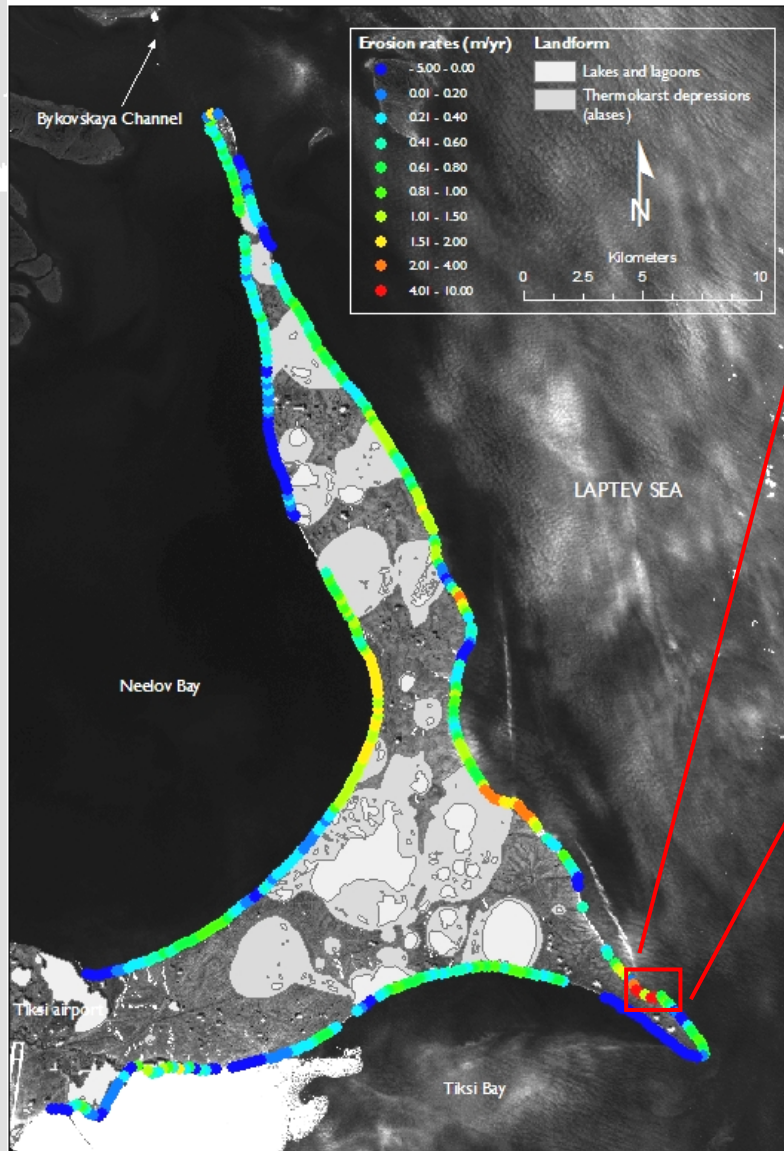
About 98% of the lakes and 14% of the water surface is not considered in current databases focusing on lakes >1 ha.



Geomorphological feature	Number	Area (km ²)	% of overall investigation area	% of Khorogor Valley	% of Bykovsky Peninsula
Thermo-erosional valleys	145	11.188	4.3	0.2	6.3
Thermokarst basins	16	80.713	31.2	-	46.1
Thermo-erosional cirques	7	1.170	0.5	-	0.7
Pingos	6	0.385	0.1	-	0.2

Erosion of the ice-rich permafrost coasts of the Bykovsky Peninsula 1951-2006

H. Lantuit, D. Atkinson, V. Rachold, M. Grigoriev, G. Grosse, S. Nikiforov

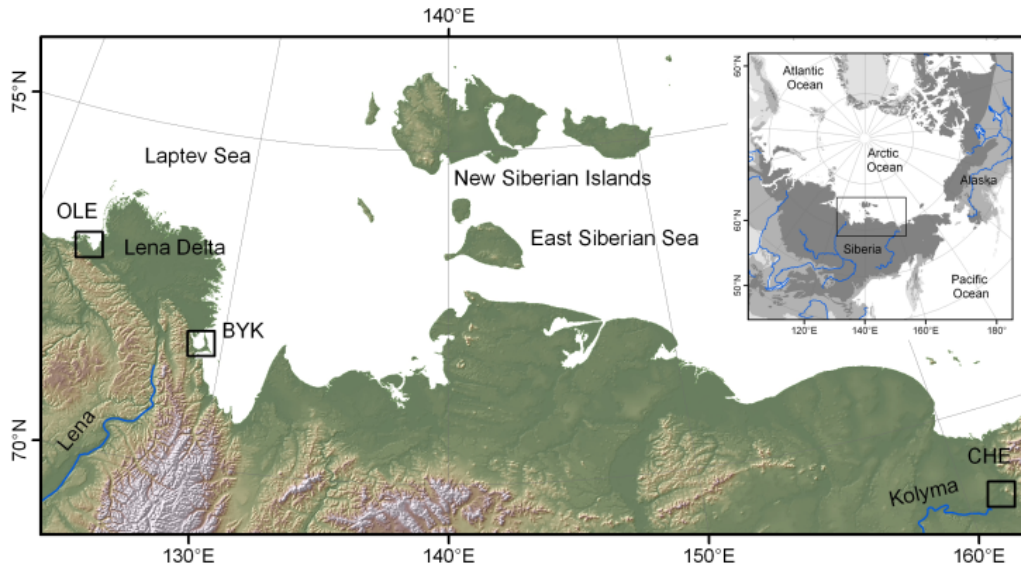


High-resolution remote sensing record for the Bykovsky Peninsula

Sensor	Ground resolution	Date
Aerial imagery	2 m	4-Aug-51
Aerial imagery	2 m	22-Jun-64
Corona KH-4B	2.5 m	24-Jun-69
Corona KH-4B	2.5 m	17-Jun-75
Hexagon KH-9	6 m	8-Aug-81
Spot-5 pan	2.5 m	9-Jul-06

Distribution and Temporal Changes of Thermokarst Lakes in Siberian Yedoma

G. Grosse, V. Romanovsky, K. Walter, A. Morgenstern, H. Lantuit, S. Zimov



Objectives

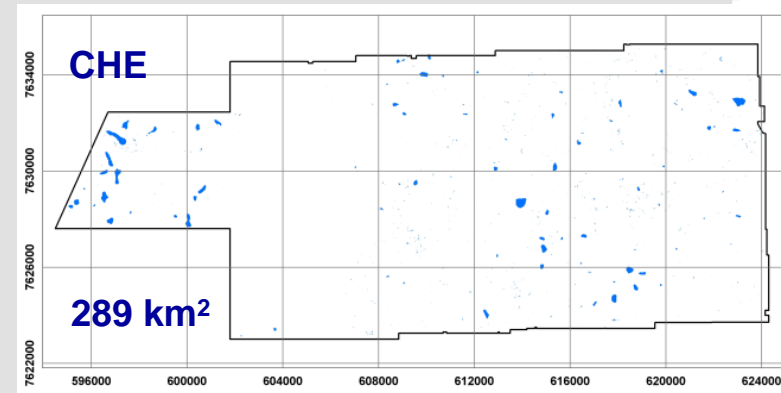
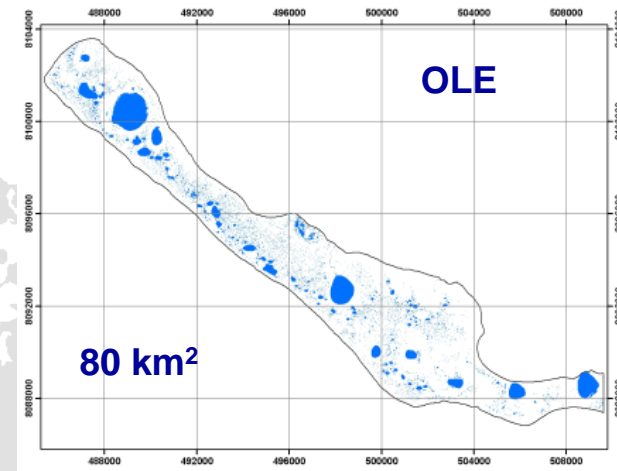
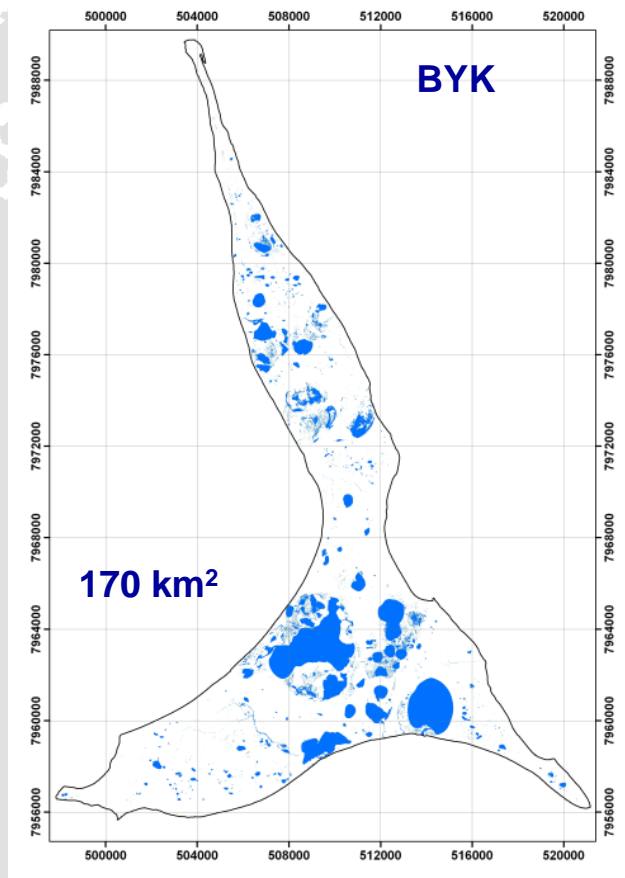
- Characterize the spatial distribution of thermokarst lakes in ice-rich permafrost areas
- Assess temporal changes over the remote sensing period

General environmental characteristics in the study regions

Study site	Cherskii (CHE)	Bykovsky (BYK)	Olenek (OLE)
Location	68.8°N/161.3°E	71.8°N/129.3°E	72.9°N/122.9°E
Permafrost depth (m)	400 – 500	500 – 600	200-600
Active layer depth (m)	0.3 – 1.5	0.3 – 0.6	0.3 – 0.6
Annual ground temperature (20 m depth)(°C)	-3 – -11	-9 – -11	-9 – -11
Annual air temperature (°C)	-12.5	-14.0	X
Annual precipitation (mm)	222	232	X
Vegetation zone	Taiga / Tundra	Tundra	Tundra
Study area (km ²)	288.97	170.09	79.82

Distribution and Temporal Changes of Thermokarst Lakes in Siberian Yedoma

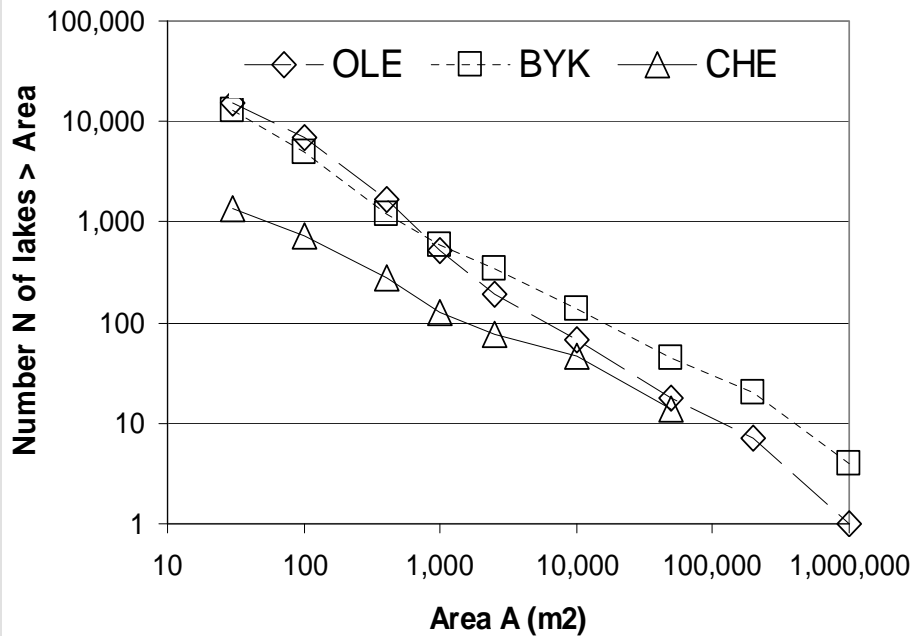
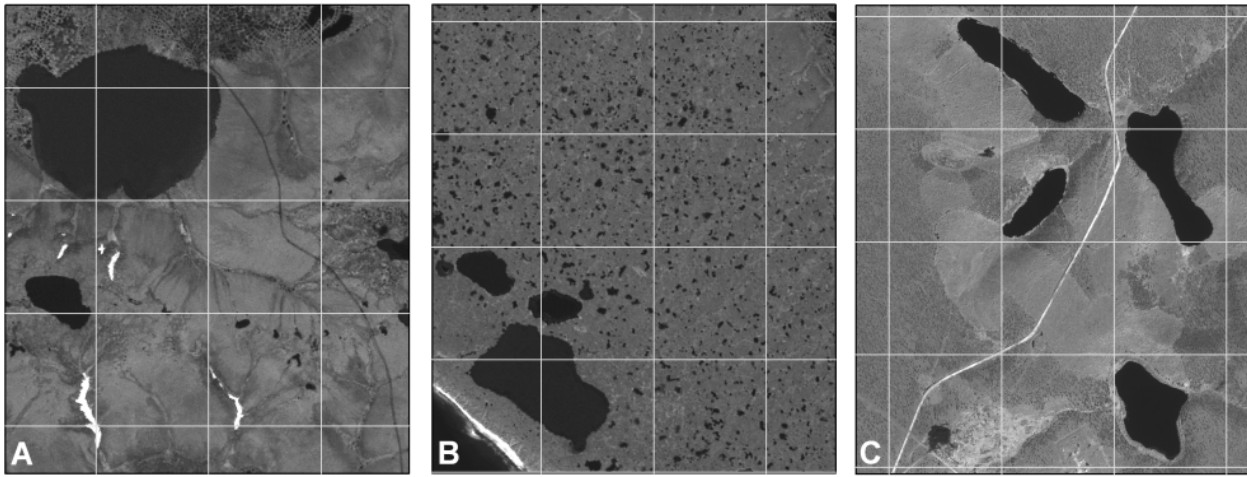
G. Grosse, V. Romanovsky, K. Walter, A. Morgenstern, H. Lantuit, S. Zimov



Parameter	OLE	BYK	CHE
Number of lakes N	15 012	13 001	1 348
Lake area A (ha)	1059.6	2622.1	242.3
Lake area A (%)	13.3	15.4	0.8
Largest lake size (ha)	196.19	605.00	16.71
Mean lake size (ha)	0.0706	0.2017	0.1797

Distribution and Temporal Changes of Thermokarst Lakes in Siberian Yedoma

G. Grosse, V. Romanovsky, K. Walter, A. Morgenstern, H. Lantuit, S. Zimov



Distribution of lakes in the study areas as the total number N of lakes larger than area A.

Distribution and Temporal Changes of Thermokarst Lakes in Siberian Yedoma

G. Grosse, V. Romanovsky, K. Walter, A. Morgenstern, H. Lantuit, S. Zimov

Table 4: Area-normalized number of lakes and lake areas

Size class (ha)	N, normalized by area (N / 100 km ²)			A, normalized by area (km ² / 100 km ²)		
	OLE	BYK	CHE	OLE	BYK	CHE
? 0.003-0.01	10 434	4 835	218	0.59	0.27	0.01
>0.01-0.04	6 332	2 102	154	1.24	0.39	0.03
>0.04-0.1	1 403	356	51	0.85	0.21	0.03
>0.1-0.25	397	152	18	0.59	0.23	0.03
>0.25-1	157	118	10	0.66	0.54	0.06
>1-5	63	54	11	1.41	1.16	0.30
>5-20	13.8	14.7	4.5	1.66	1.62	0.38
>20-100	7.5	9.4	0	3.83	3.54	0
>100-1 000	1.3	2.4	0	2.46	7.47	0

Table 2: Overview of remote sensing imagery used for lake area change detection

Site	Platform	Date	Ground Resolution	Spectral properties	RMS error	No. GCP	Transformation method
BYK	Corona KH-4B	1969-06-24	2.5 m	Panchromatic	4.58m / 3.42m	37 / 29	NN, 3rd polynomial
BYK	Spot-5	2006-07-09	2.5 m	Panchromatic	Base	-	-
OLE	Corona KH-4A	1964-06-22	2.5 m	Panchromatic	1.18m / 4.53m	14 / 38	NN, 3rd polynomial
OLE	Spot-5	2006-07-08	2.5 m	Panchromatic	Base	-	-
CHE	Gambit KH-7	1965-10-01	1 m	Panchromatic	3.06m	28	NN, 3rd polynomial
CHE	Ikonos-2	2002-07-09	1 m	Panchromatic	Base	-	-

Distribution and Temporal Changes of Thermokarst Lakes in Siberian Yedoma

G. Grosse, V. Romanovsky, K. Walter, A. Morgenstern, H. Lantuit, S. Zimov

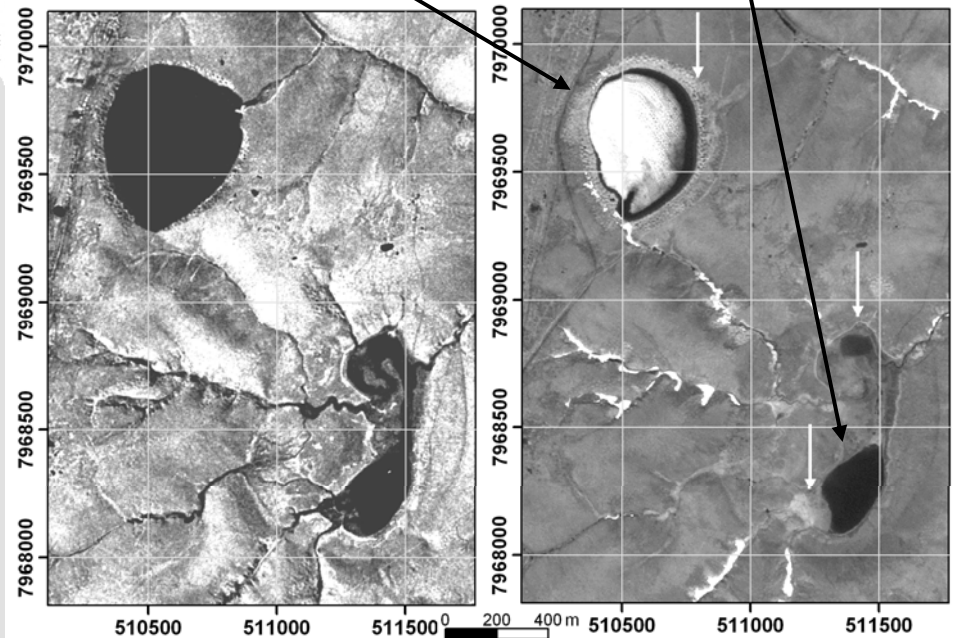
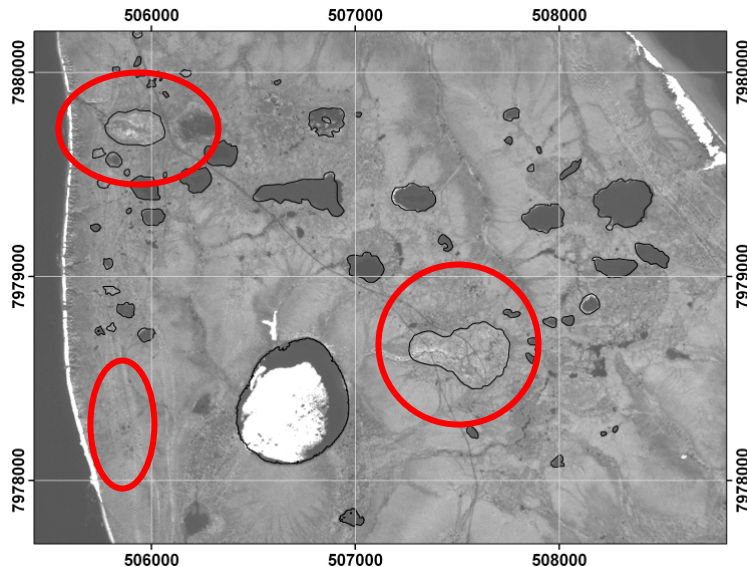
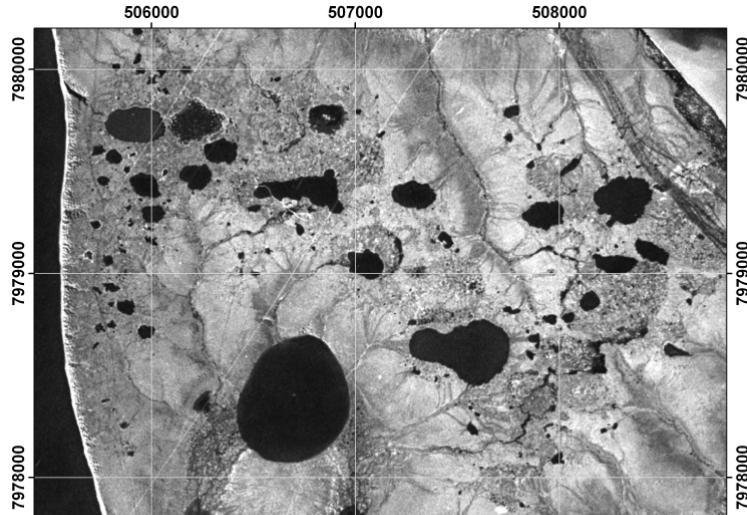
Bykovsky Peninsula

(Corona KH-4B 1969 vs. Spot-5 2002)

(2.5m ground resolution)

Lake shrinkage by 7.56 ha (-28.5 %)

Lake shrinkage by 6.97 ha (-53.2 %)



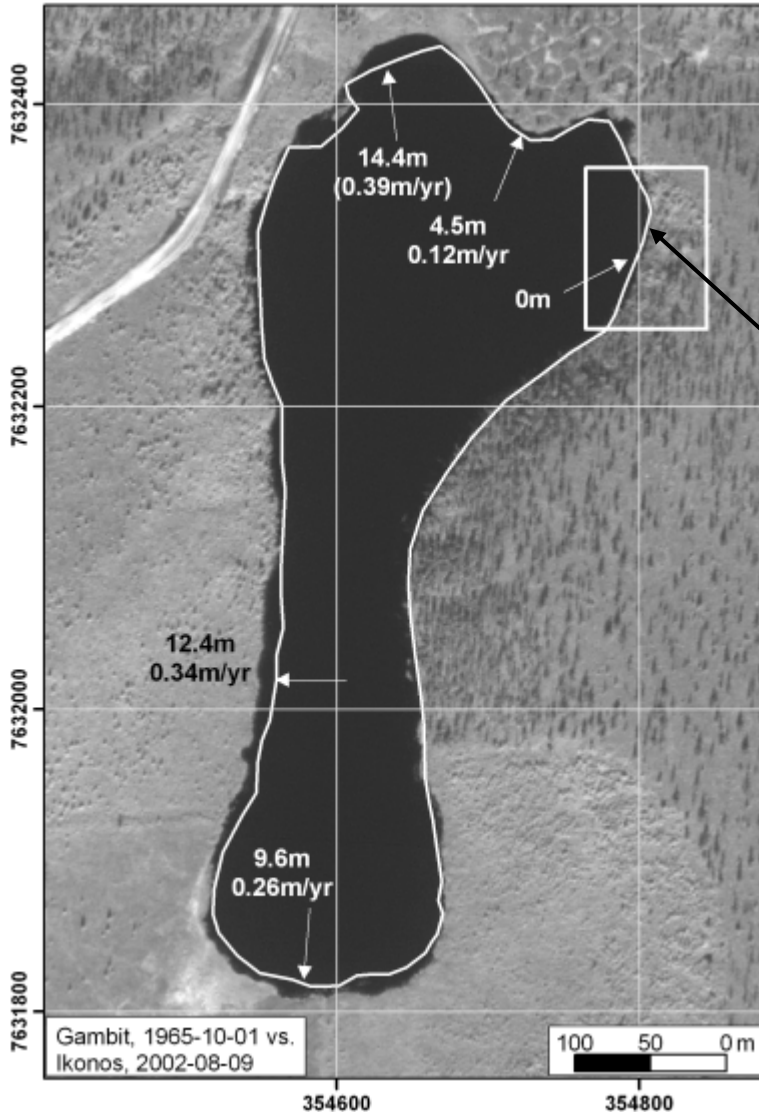
- Of 308 arbitrary selected lakes, 244 indicate shrinkage, 44 growth, and 20 lakes drained completely

- Net shrinkage is 24.4 ha (-2.9%)

Distribution and Temporal Changes of Thermokarst Lakes in Siberian Yedoma

G. Grosse, V. Romanovsky, K. Walter, A. Morgenstern, H. Lantuit, S. Zimov

Thermo-erosion along shore bluffs of thermokarst lakes in the Cherskii region (Gambit 1965 vs. Ikonos-2 2002) (1.0 m ground resolution)

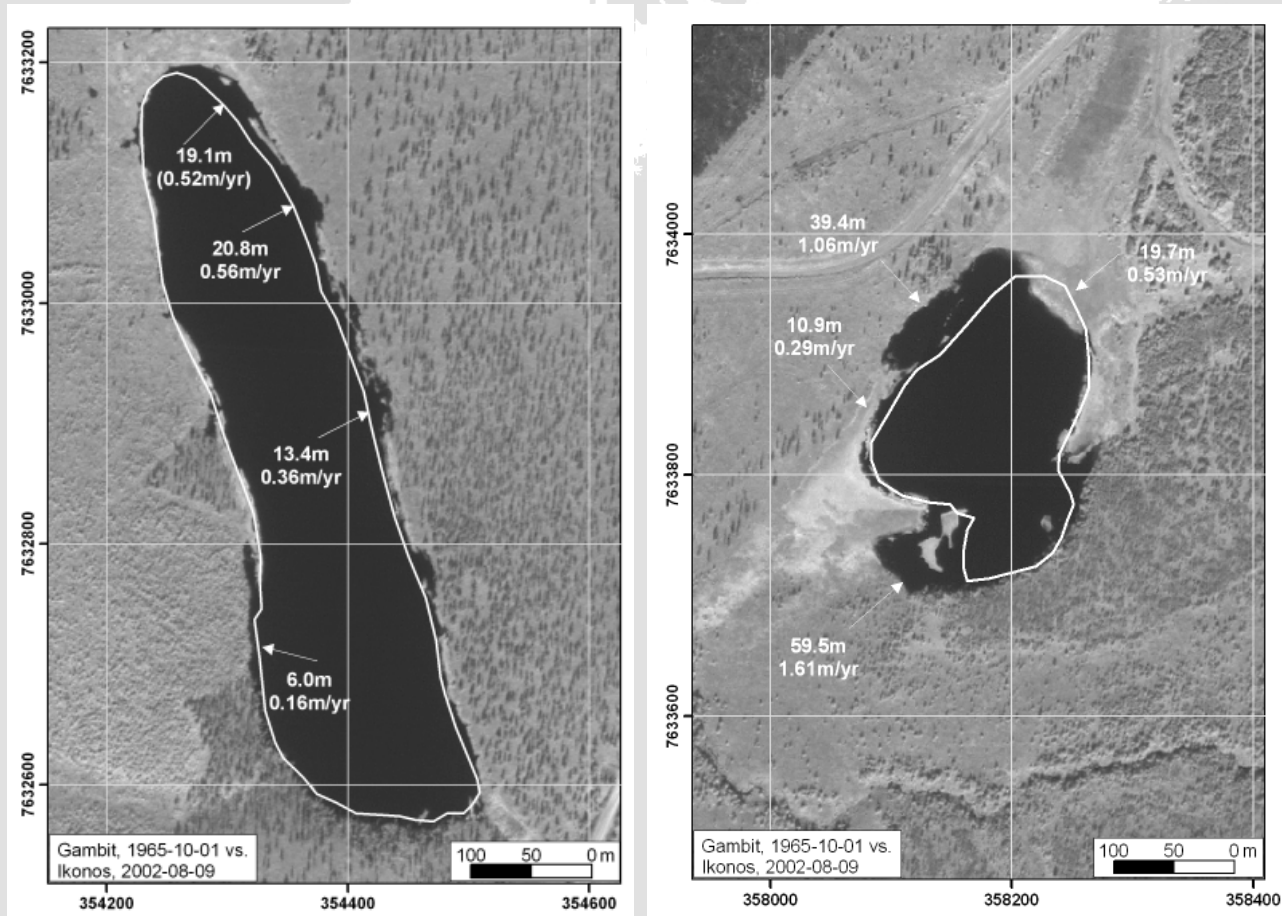


September 2007

Distribution and Temporal Changes of Thermokarst Lakes in Siberian Yedoma

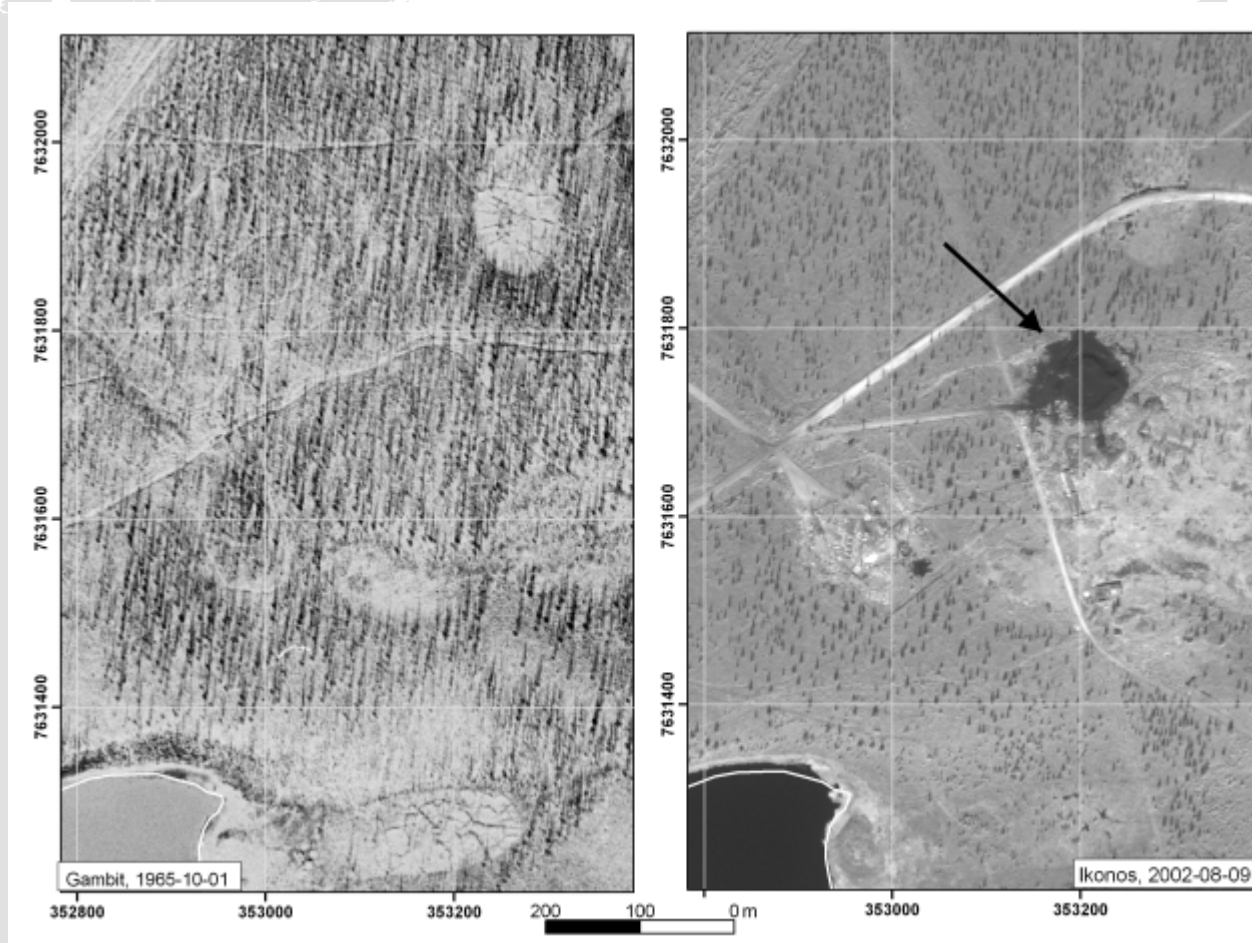
G. Grosse, V. Romanovsky, K. Walter, A. Morgenstern, H. Lantuit, S. Zimov

*Thermo-erosion along shore bluffs of thermokarst lakes
(Gambit 1965 vs. Ikonos-2 2002) (1.0 m ground resolution)*



Human impact on permafrost

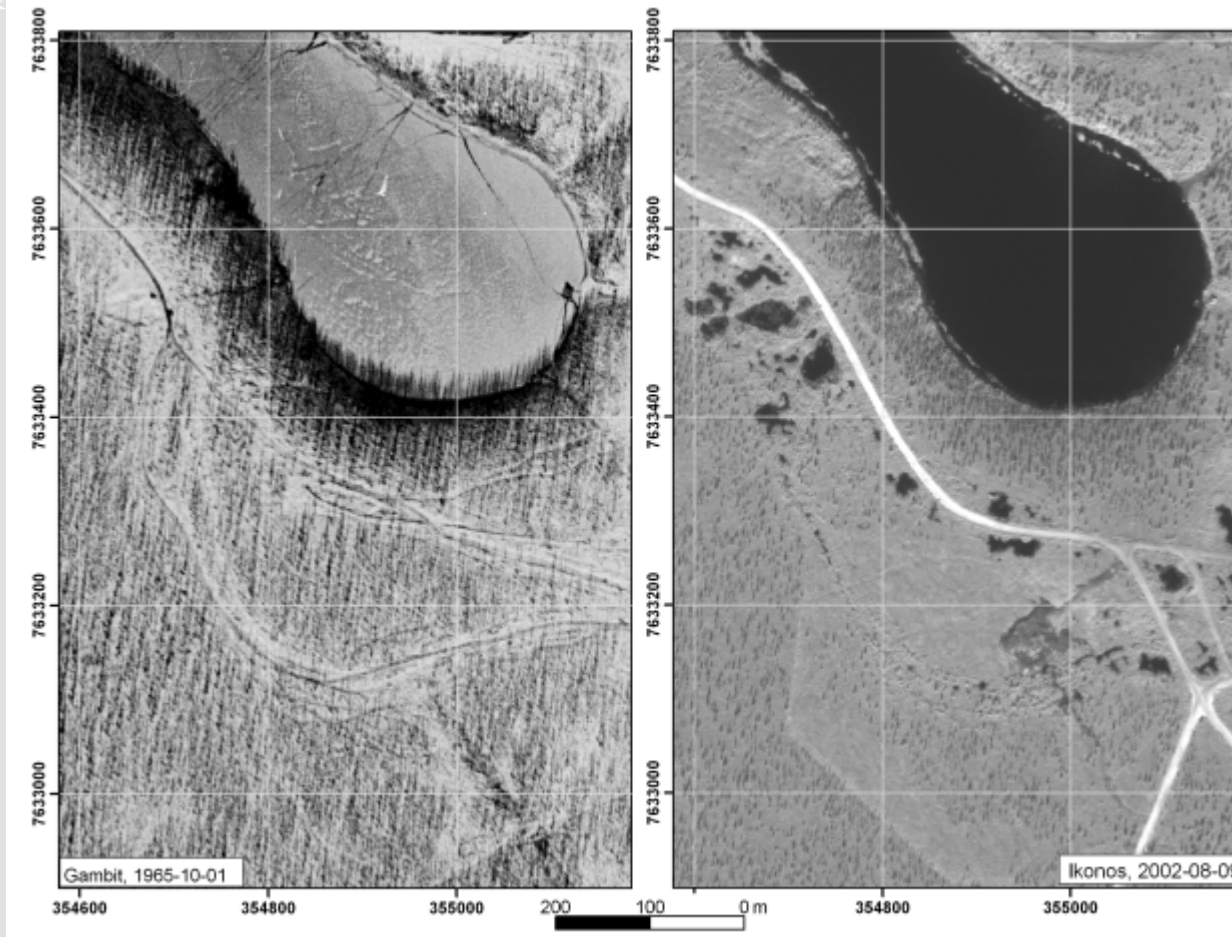
Increase of surface wetness due to initial thermokarst at a former construction site, Cherskii (Russia)



(Gambit 1965 vs. Ikonos-2 2002) (1.0 m ground resolution)

Human impact on permafrost

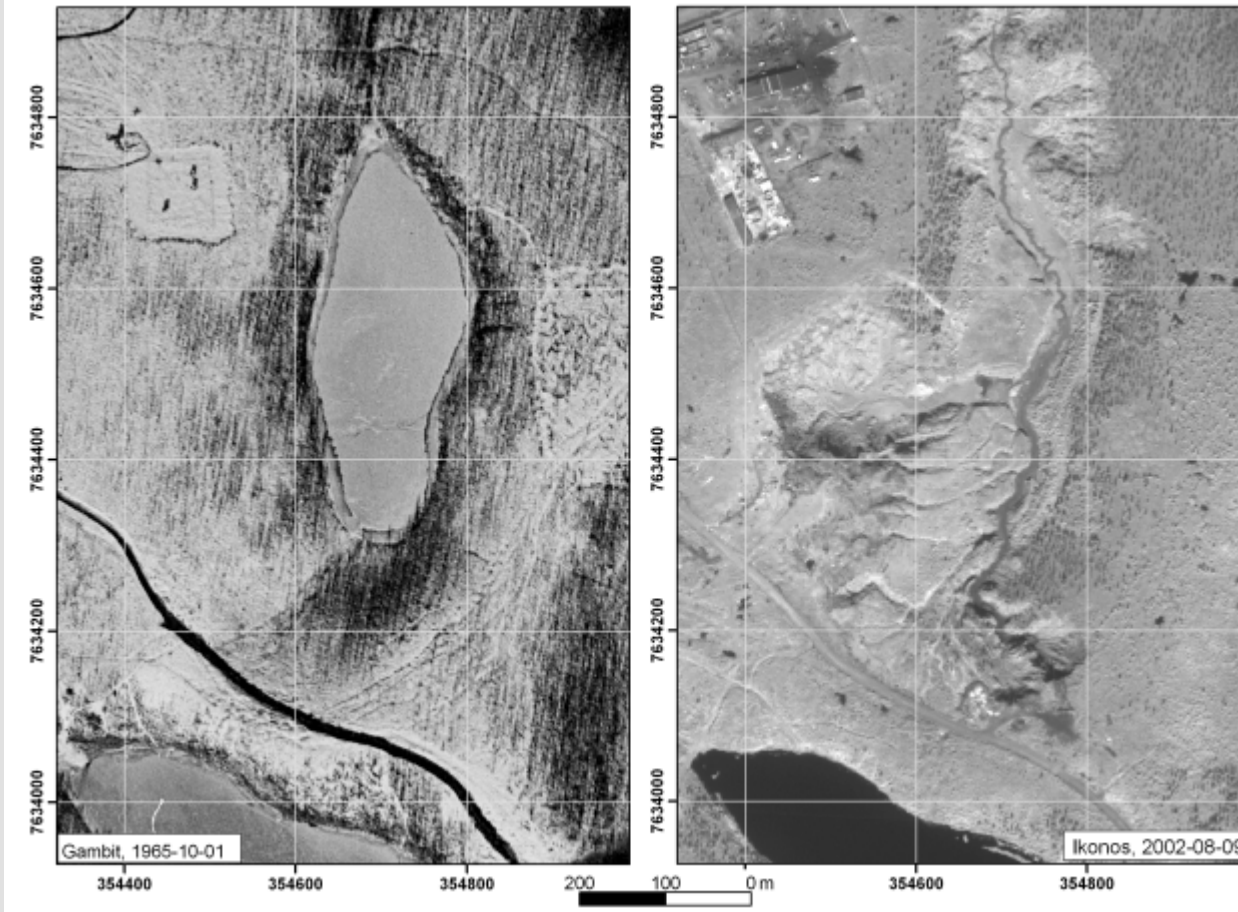
*Massive thermokarst pond formation along former dirt roads,
Cherskii (Russia)*



(Gambit 1965 vs. Ikonos-2 2002) (1.0 m ground resolution)

Human impact on permafrost

*Artificial drainage of a thermokarst lake,
followed by the formation of retrogressive thaw slumps, Cherskii (Russia)*



(Gambit 1965 vs. Ikonos-2 2002) (1.0 m ground resolution)

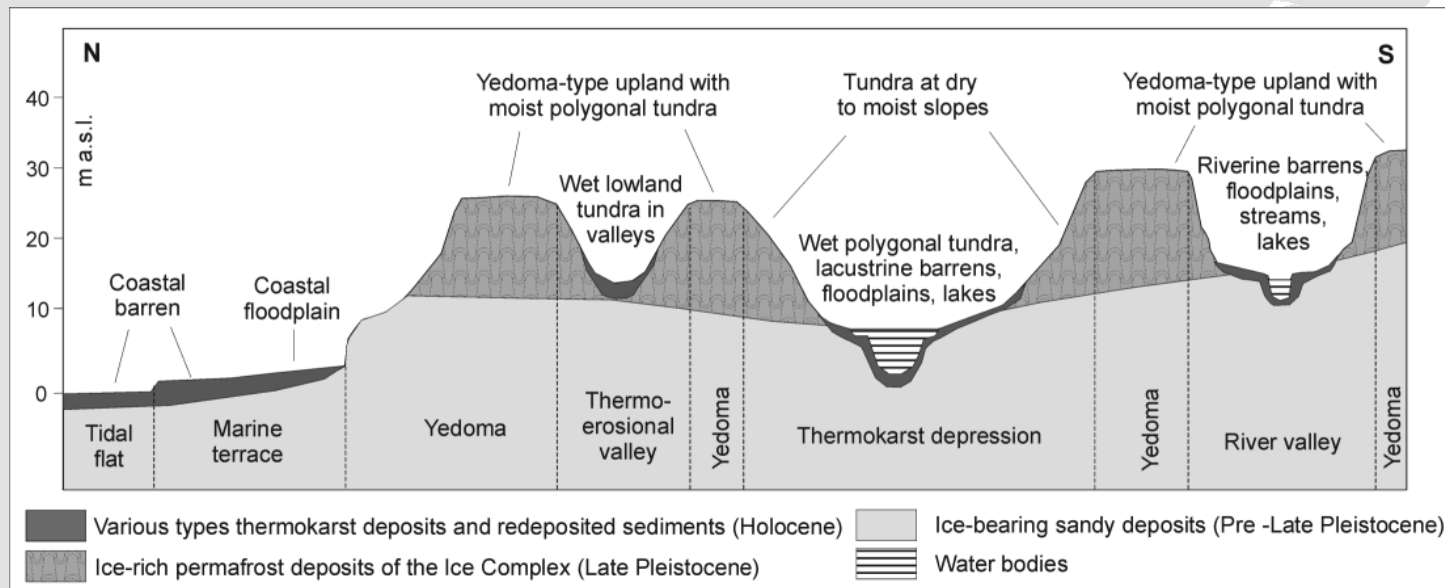
Classification of Thermokarst-Affected Terrain with Landsat-7 data and a DEM

G. Grosse, L. Schirrmeister, T. Malthus



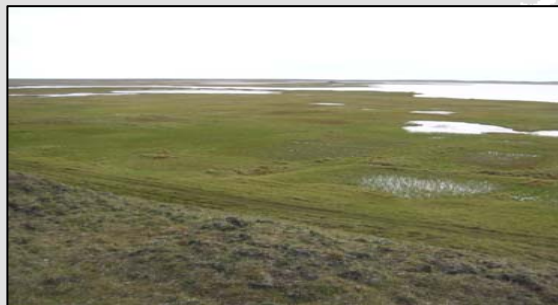
Study site: Cape Mamontov Klyk

- Large scale study site: 3400 km²
- DEM with 30 m grid cell size
- 1 Landsat-7 ETM+ image + 4 Corona images
- Cryolithological data from outcrop profiles
- Surface data from 179 sites:
 - Macro-, Meso- and Micro- relief forms, relief position, slope inclination, surface / vegetation cover, water bodies and soil moisture, morphometric measurements, active layer depth

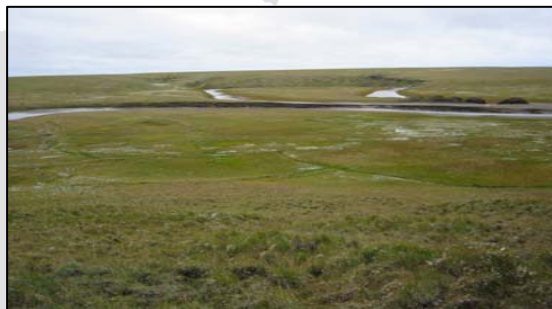


Classification of Thermokarst-Affected Terrain with Landsat-7 data and a DEM

G. Grosse, L. Schirrmeister, T. Malthus



Wet polygonal tundra in thermokarst basin



Riverine floodplain with polygonal tundra



Moist, Edoma-type upland tundra



Wet lowland tundra in thermokarst valleys



Riverine barren, Fluvial sand terrace

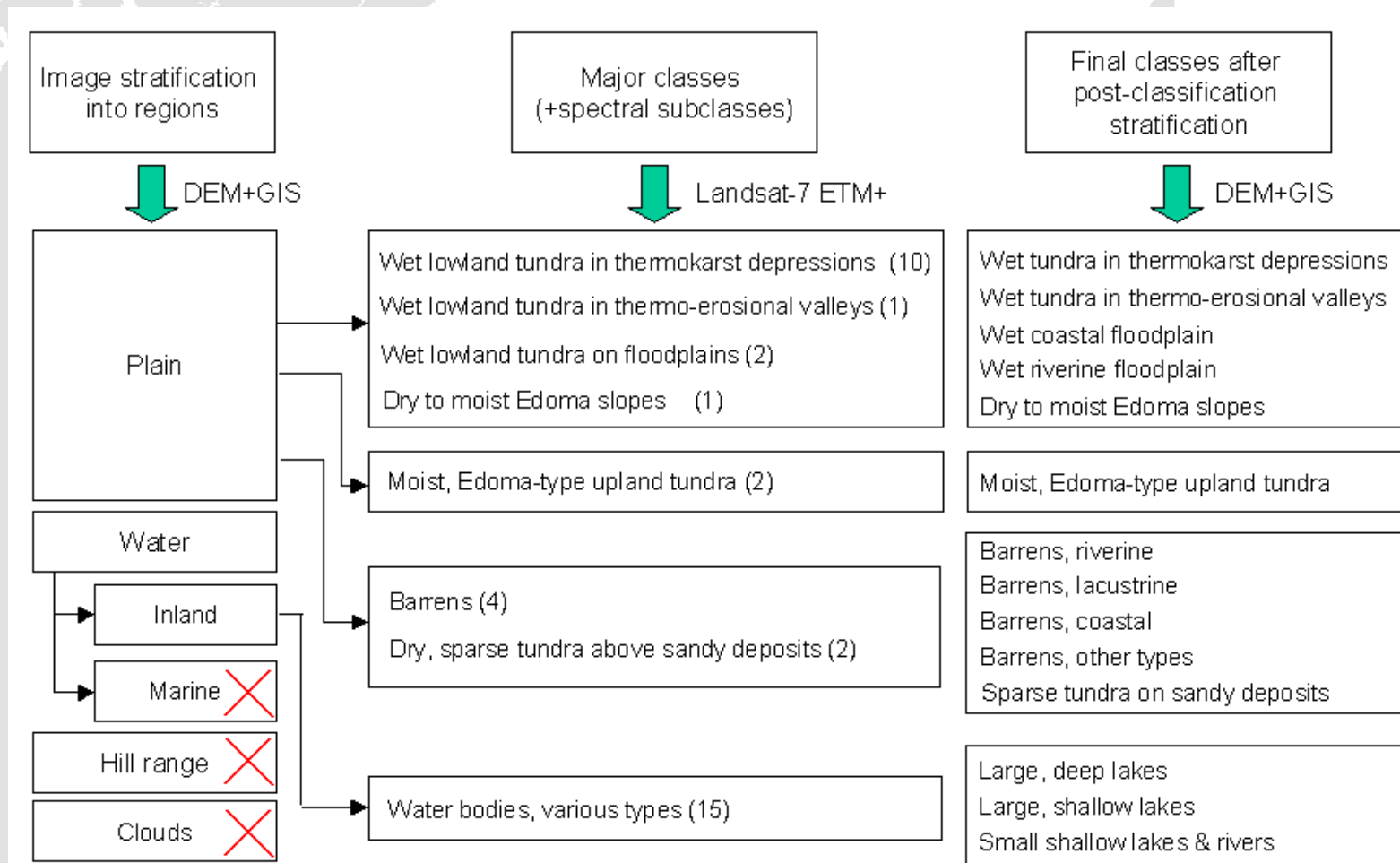


Dry slopes with thermokarst hills

Classification of Thermokarst-Affected Terrain with Landsat-7 data and a DEM

G. Grosse, L. Schirrmeister, T. Malthus

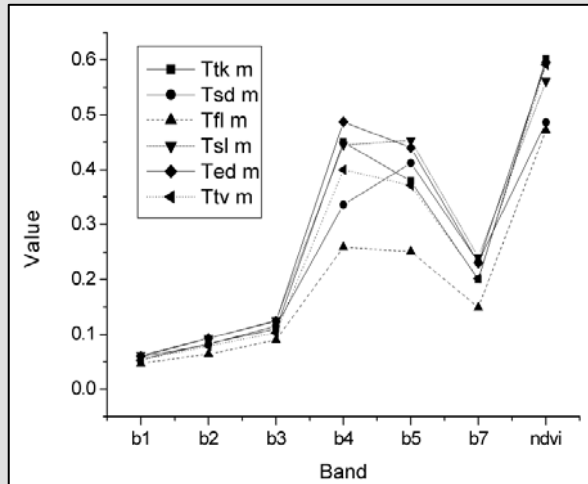
Classification approach



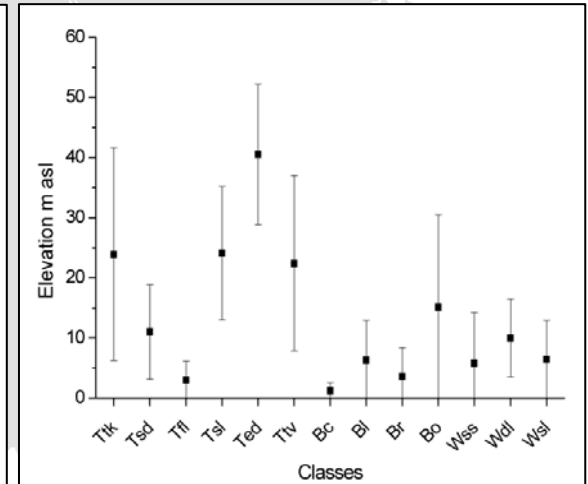
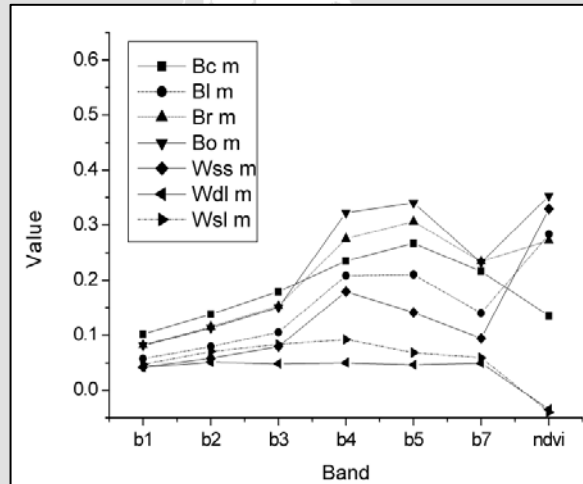
Classification of Thermokarst-Affected Terrain with Landsat-7 data and a DEM

G. Grosse, L. Schirrmeister, T. Malthus

Mean values for each class



Spectral bands + NDVI



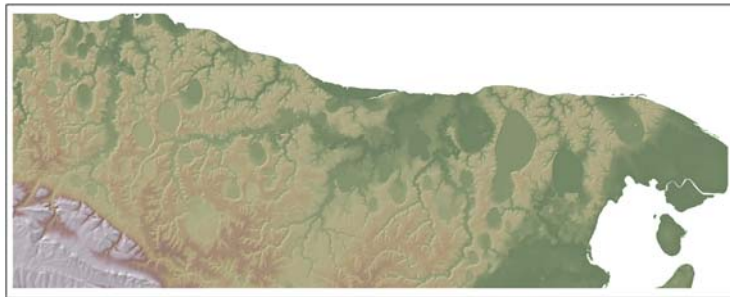
Surface elevation

Classification of Thermokarst-Affected Terrain with Landsat-7 data and a DEM

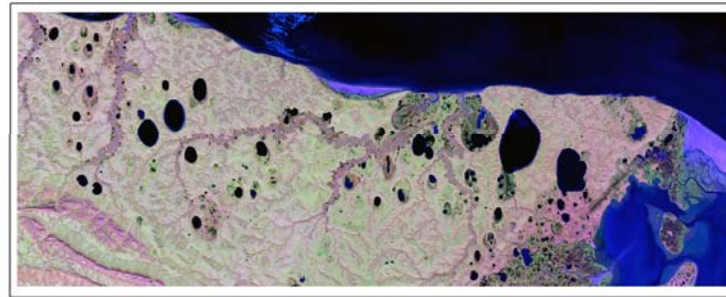
G. Grosse, L. Schirrmeyer, T. Malthus

0 5 10 20 30 40 50 Kilometers

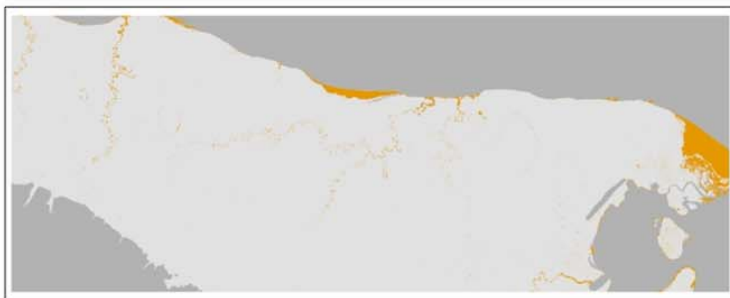
0 5 10 20 30 40 50 Kilometers



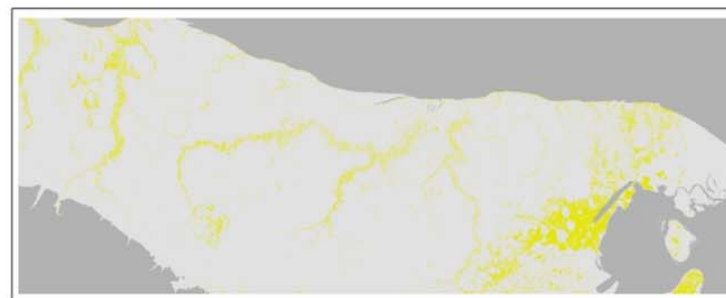
DEM



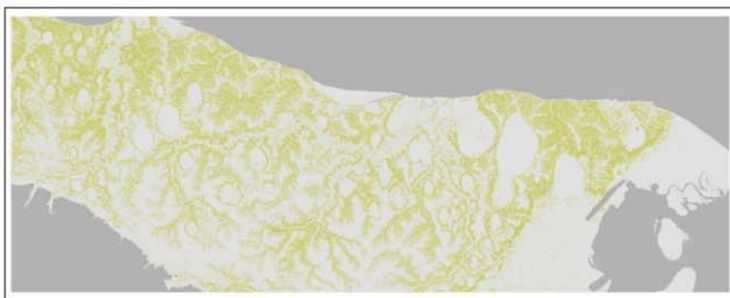
Landsat-7 data, bands 5-4-3



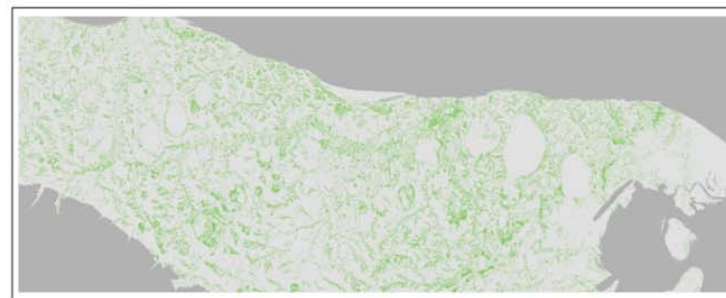
Barrens, various types



Dry, sparse tundra above sandy deposits



Dry to moist tundra at slopes



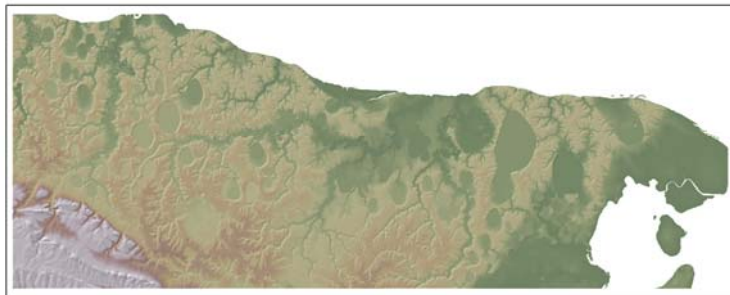
Wet lowland tundra in thermo-erosional valleys

Classification of Thermokarst-Affected Terrain with Landsat-7 data and a DEM

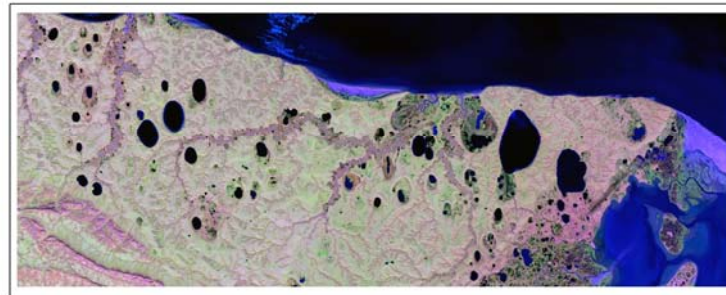
G. Grosse, L. Schirrmeister, T. Malthus

0 5 10 20 30 40 50 Kilometers

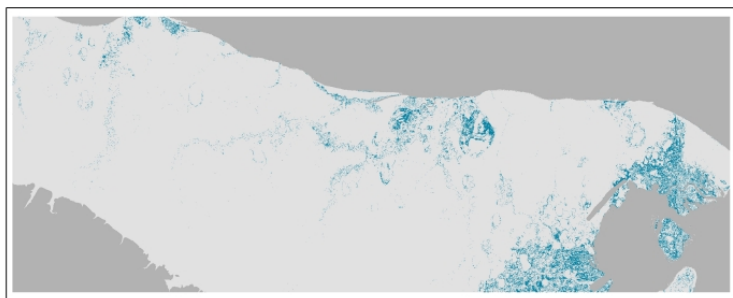
0 5 10 20 30 40 50 Kilometers



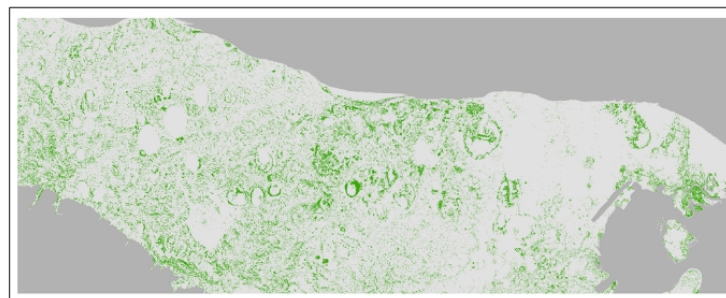
DEM



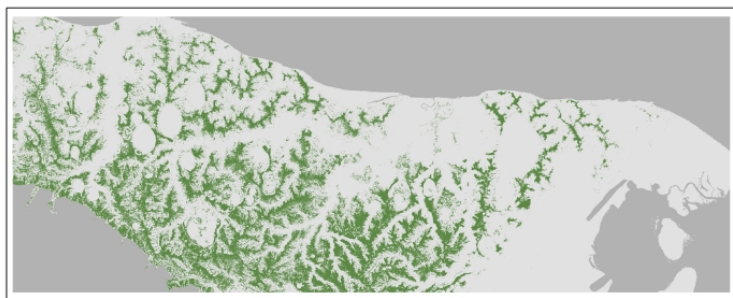
Landsat-7 data, bands 5-4-3



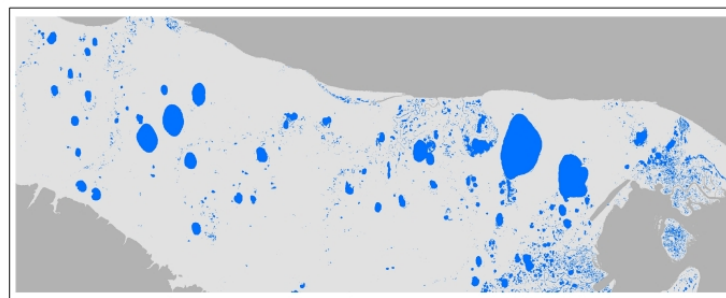
Wet lowland tundra in floodplains



Wet lowland tundra in thermokarst depressions



Wet, Edoma-type upland tundra

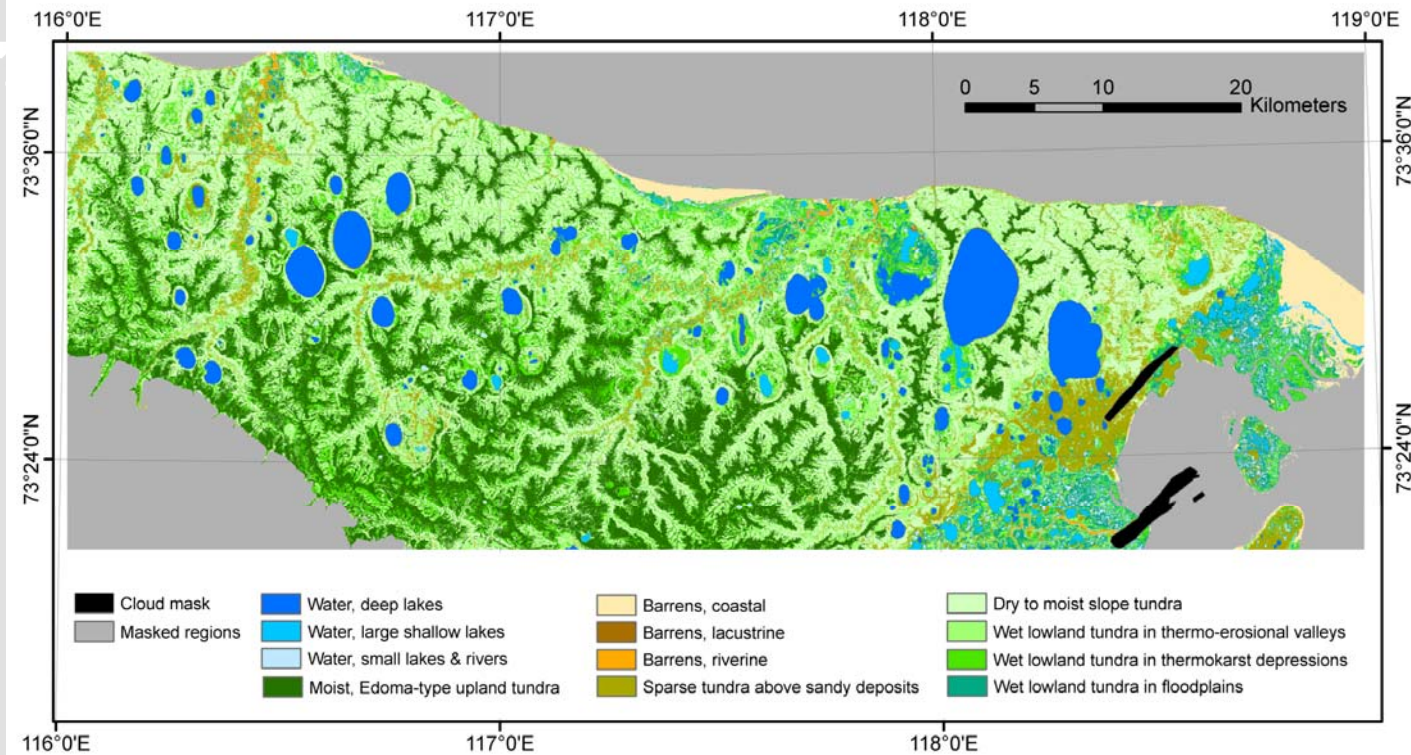


Water, various types



Classification of Thermokarst-Affected Terrain with Landsat-7 data and a DEM

G. Grosse, L. Schirrmeister, T. Malthus



Assumption based on field data: All of the coastal plain was covered by ice-rich deposits.

Degree of thermokarst degradation for the coastal plain (=2317.5 sqkm)

22.2 % No degradation of ice-rich deposits

31.1 % Partial degradation of ice-rich deposits

14.7 % Strong degradation of ice-rich deposits

11.4 % Complete degradation of ice-rich deposits

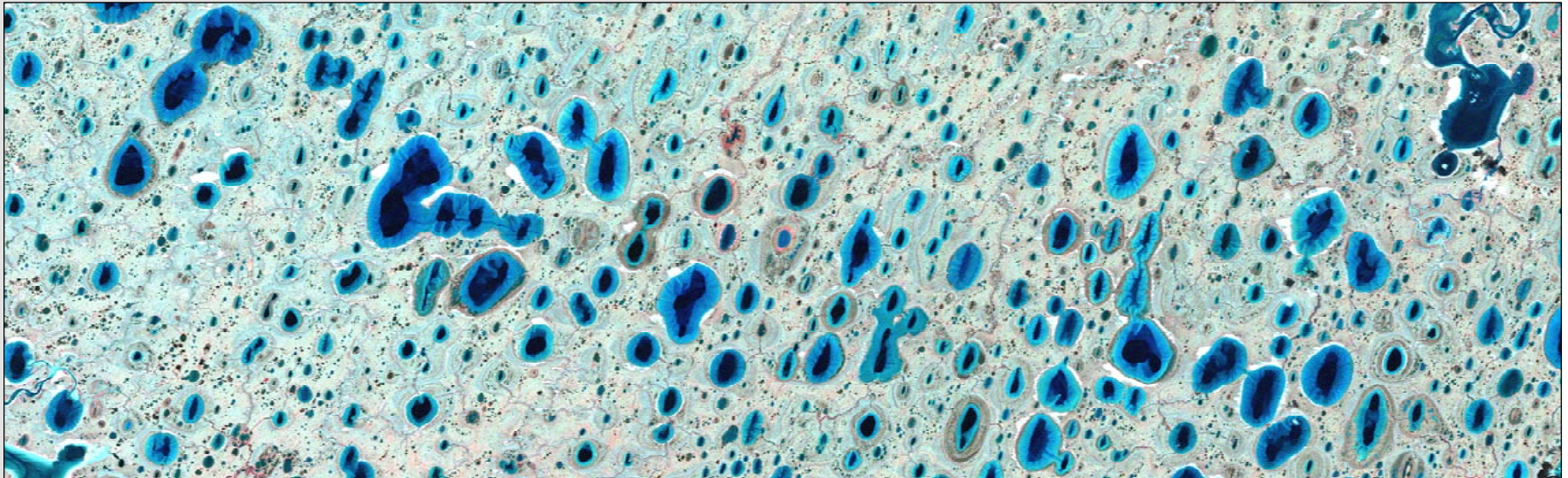
20.6 % Complete degradation of ice-rich deposits + deeper deposits

Morphometry and spatial distribution of lakes in the Lena Delta

A. Morgenstern, G. Grosse, L. Schirrmeyer

Goals:

- *Development of a detailed GIS-based lake inventory for the largest Arctic River Delta*
- *Analysis of morphometric lake parameters for lake classification (lake genesis, phenomenon of lake orientation)*
- *Investigation of relationship between lake morphometry and environmental properties (cryolithology, geomorphology, weather patterns)*



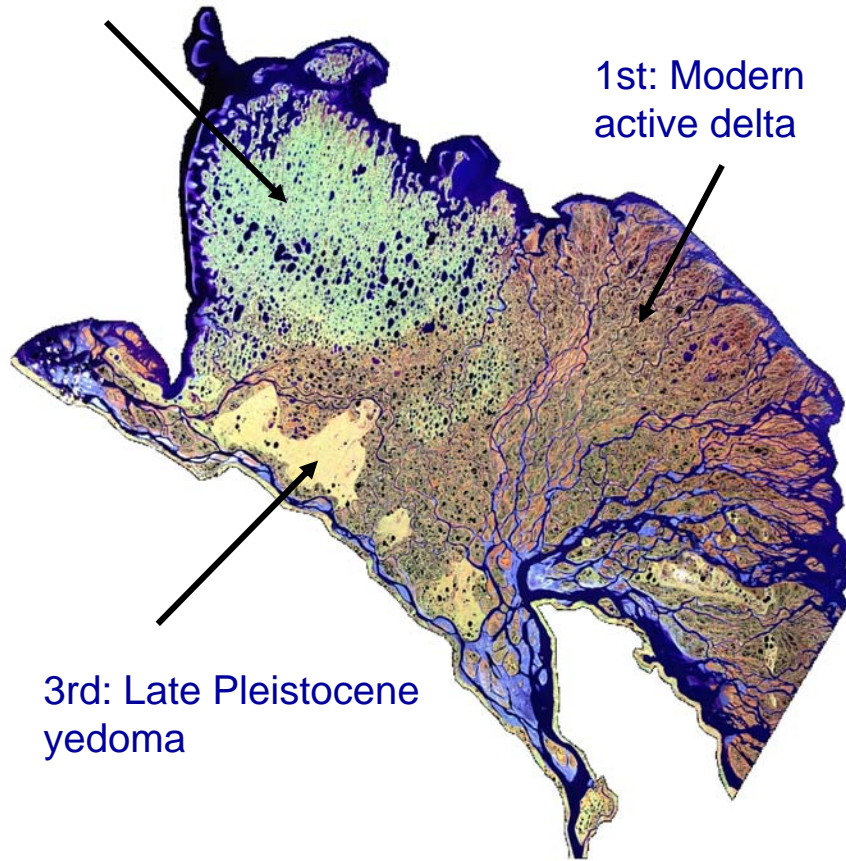
Morphometry and spatial distribution of lakes in the Lena Delta

A. Morgenstern, G. Grosse, L. Schirrmeister

2nd: Late Pleistocene – Early Holocene, fluvial sands

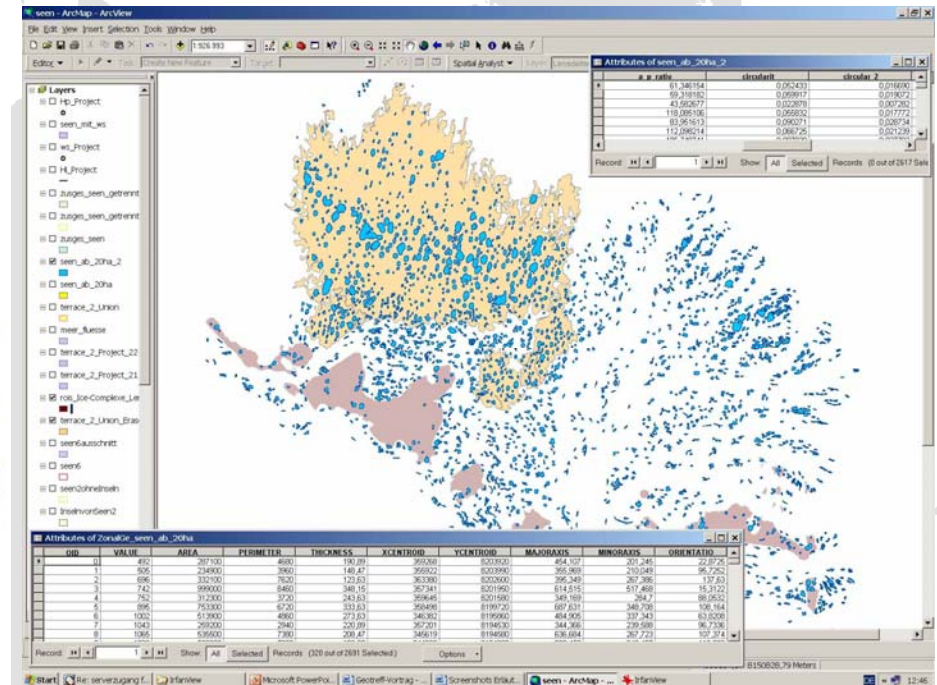
1st: Modern active delta

3rd: Late Pleistocene yedoma



Landsat-7 ETM+ mosaic (Schneider, 2005)

- Remote sensing data used: Landsat-7 ETM+
- Land-water classification based on band 5 (SWIR)
- Lakes >20ha are considered in the database



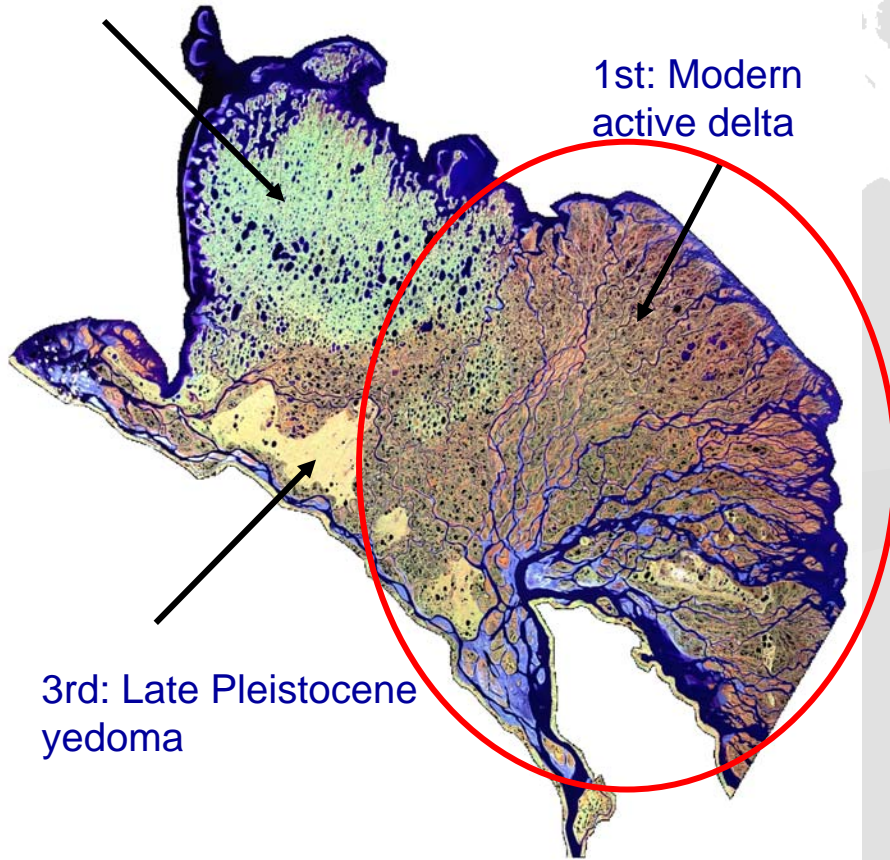
Morphometry and spatial distribution of lakes in the Lena Delta

A. Morgenstern, G. Grosse, L. Schirrmeister

2nd: Late Pleistocene – Early
Holocene, fluvial sands

1st: Modern
active delta

3rd: Late Pleistocene
yedoma



Landsat-7 ETM+ mosaic (Schneider, 2005)

Mean lake types

- *small*
- *irregular shape*
- *strong deviations from mean orientation*
- *often oxbows*

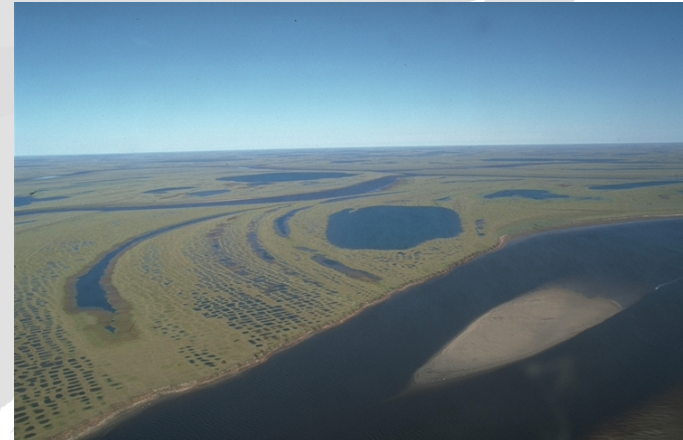
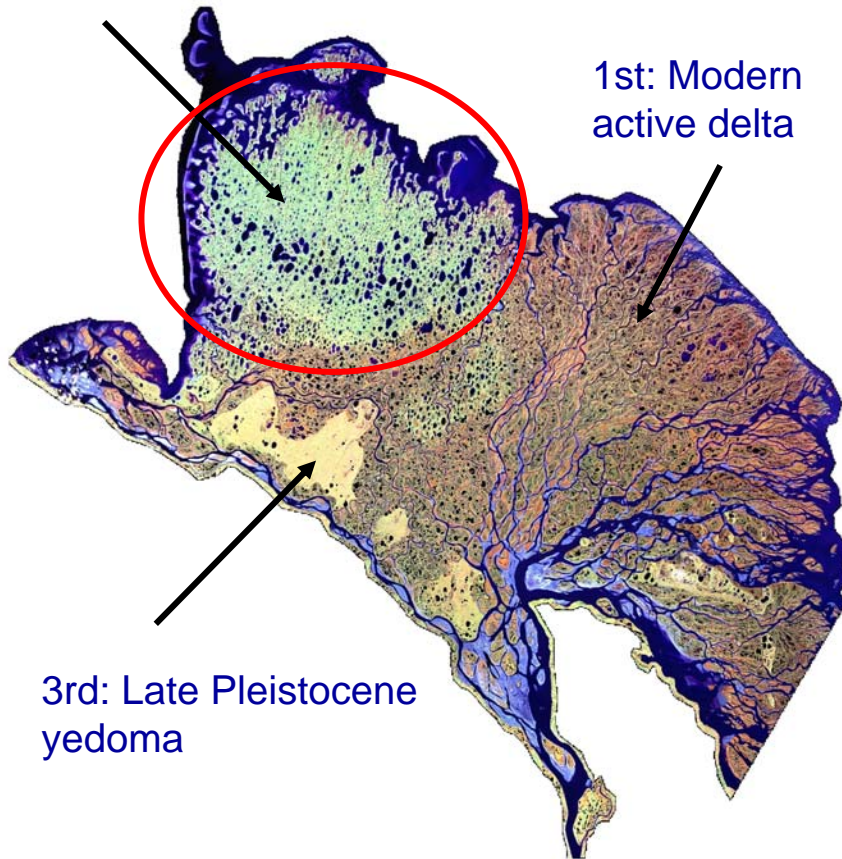


photo: AWI Potsdam

Morphometry and spatial distribution of lakes in the Lena Delta

A. Morgenstern, G. Grosse, L. Schirrmeister

2nd: Late Pleistocene – Early
Holocene, fluvial sands



Landsat-7 ETM+ mosaic (Schneider, 2005)

Mean lake types

- *large*
- *elongated*
- *NNE orientation*
- *probably secondary thermokarst lakes*

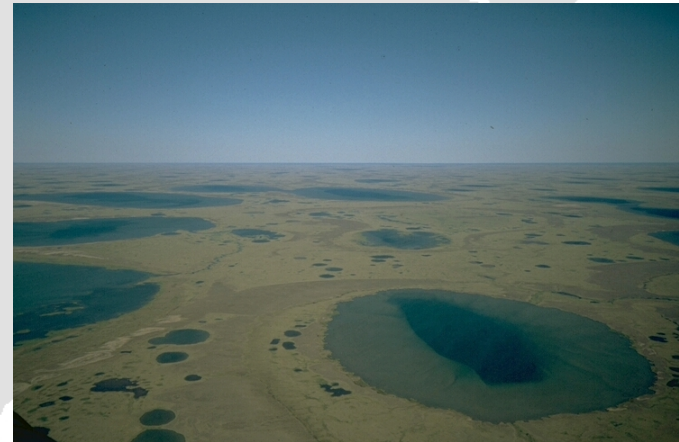


photo: V. Rachold

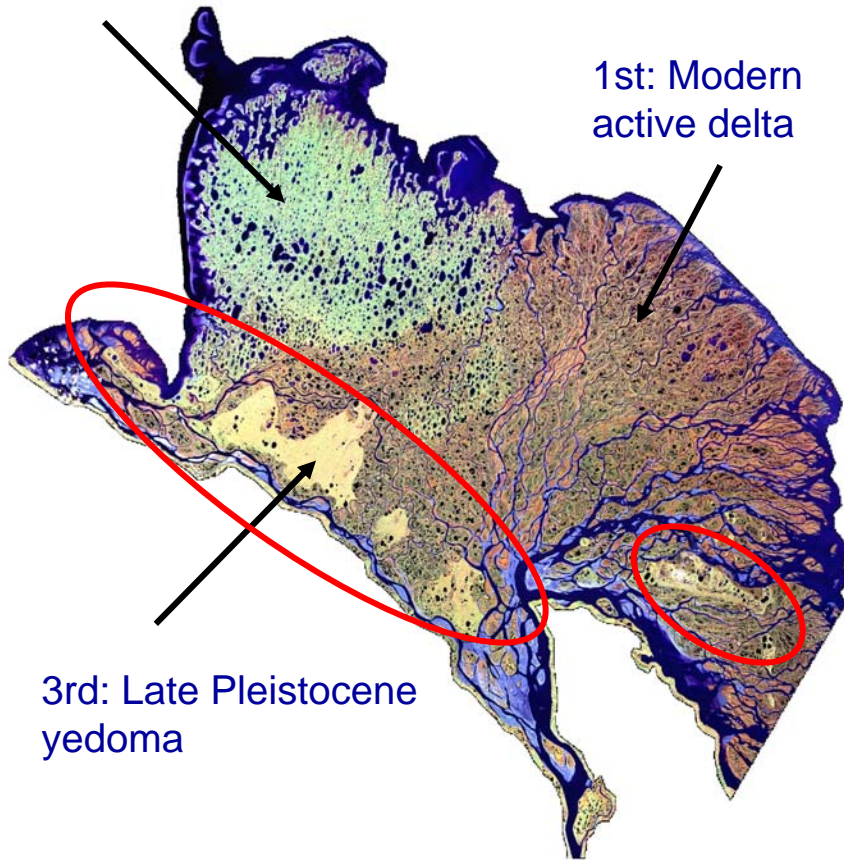
Morphometry and spatial distribution of lakes in the Lena Delta

A. Morgenstern, G. Grosse, L. Schirrmeister

2nd: Late Pleistocene – Early
Holocene, fluvial sands

1st: Modern
active delta

3rd: Late Pleistocene
yedoma



Landsat-7 ETM+ mosaic (Schneider, 2005)

Mean lake types

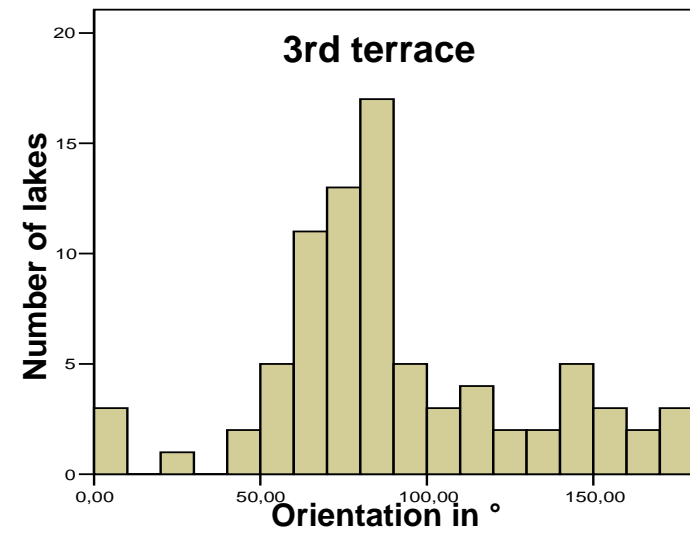
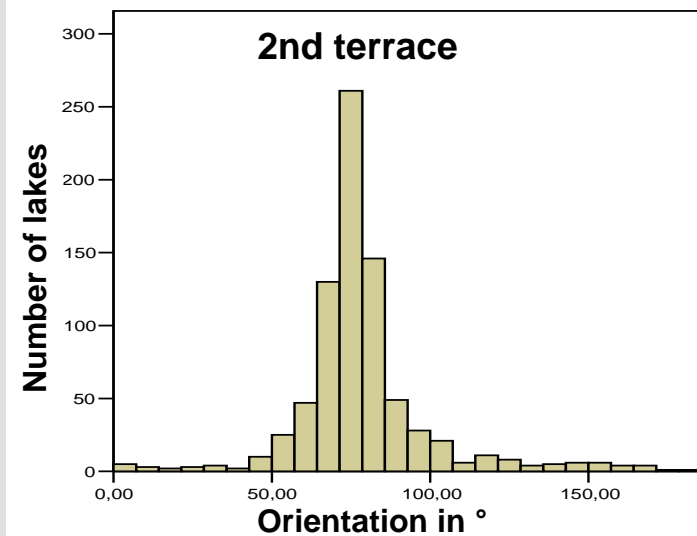
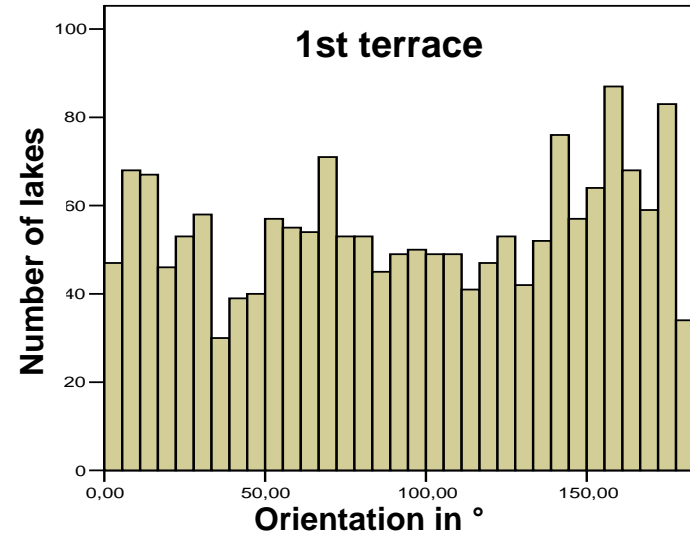
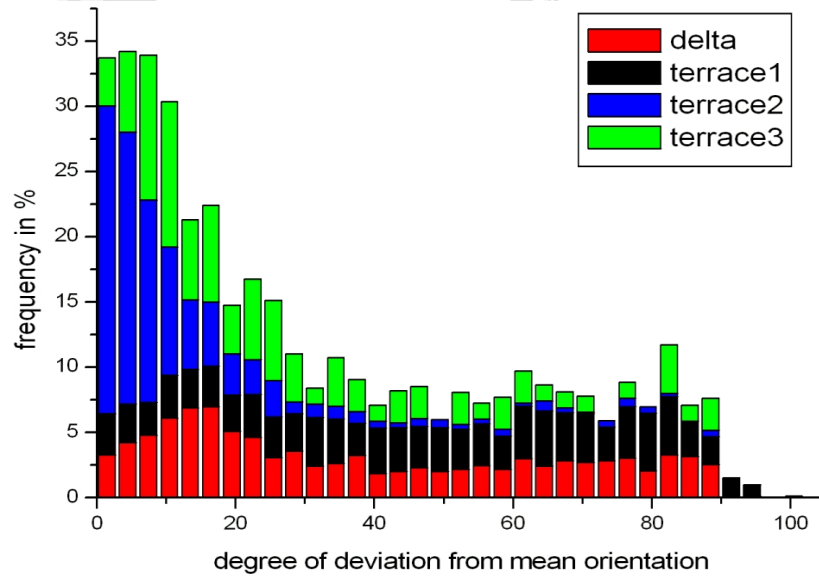
- *near circular*
- *regular shorelines*
- *primary thermokarst lakes*



photo: M. Krbetschek

Morphometry and spatial distribution of lakes in the Lena Delta

A. Morgenstern, G. Grosse, L. Schirrmeister



Morphometry and spatial distribution of lakes in the Lena Delta

A. Morgenstern, G. Grosse, L. Schirrmeister

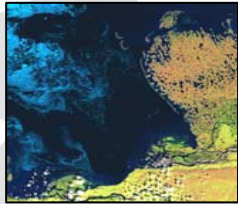
Results

- *main terraces vary strongly in the morphometric characteristics of their lakes*
- *lithology / cryolithology strongly control orientation processes*
- *active fluvial processes inhibit orientation processes on the 1st terrace*
- *since the same exogenous factors influence the 2nd and 3rd terraces, different lithology and cryolithology are the main driver for a different response to orienting forces*
- *oriented lakes on the 2nd terrace:*
 - *mean orientation = 79° (NNE-SSW)*
 - *63% with deviation from mean orientation $\leq 10^\circ$*

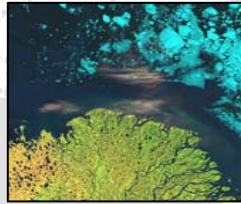
Methane Fluxes from Periglacial Landscapes in the Lena River Delta

J. Schneider, G. Grosse, D. Wagner

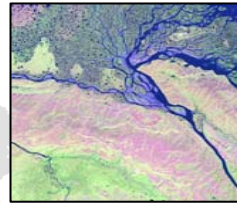
26. July 2001



27. July 2000



27. July 2000



Landsat 7 ETM+
satellite images

Rectification, resampling, radiometric correction,
image-based atmospheric correction

Local thematic maps, field reports,
aerial and field photography

Image mosaic of the Lena Delta

Selected training areas
(34 for 9 land cover classes)

Supervised land cover classification of bands
1-5 and 7, based on minimum distance algorithm

**Methane balance
of the Lena Delta**

Helicopter-based
aerial RGB image
from main study site
Samoylov Island

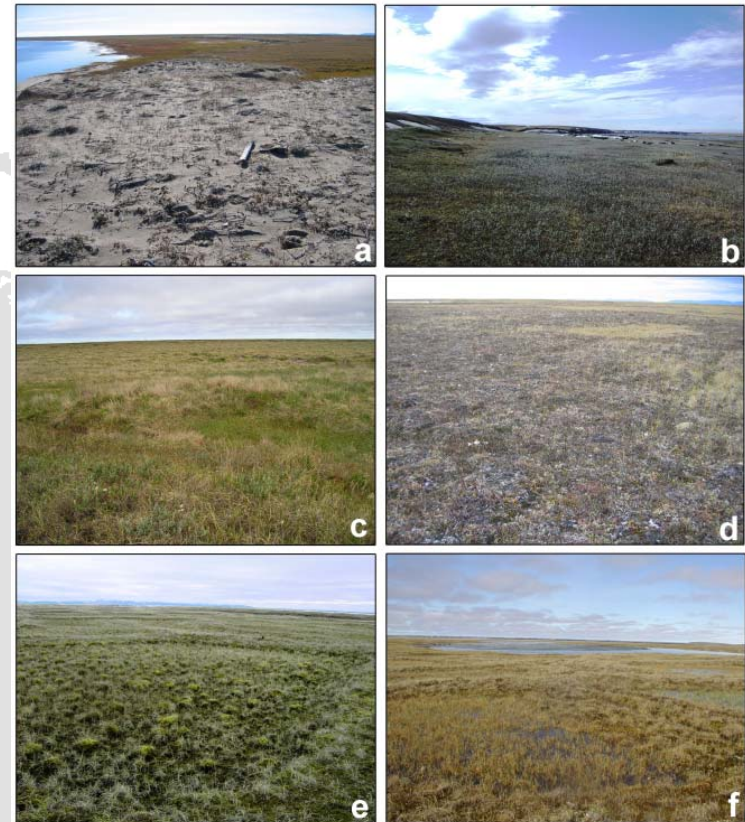
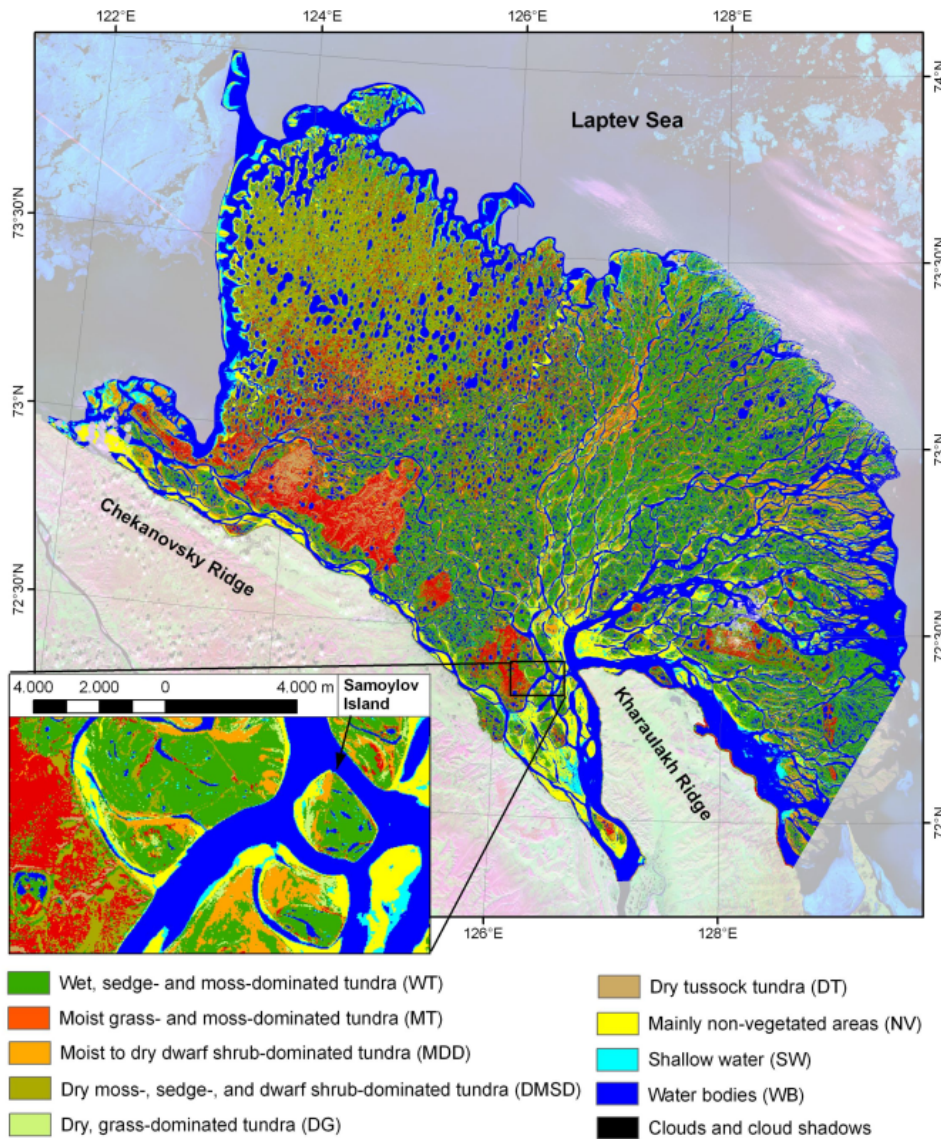
High-resolution habitat characterization
(maximum likelihood supervised classification)

Methane closed chamber measurements in various habitats
(1999-2006). Methane concentration measured with gas
chromatograph in the field laboratory (Wagner et al., 2003)

Published methane
emission
results for some
habitat types

Methane Fluxes from Periglacial Landscapes in the Lena River Delta

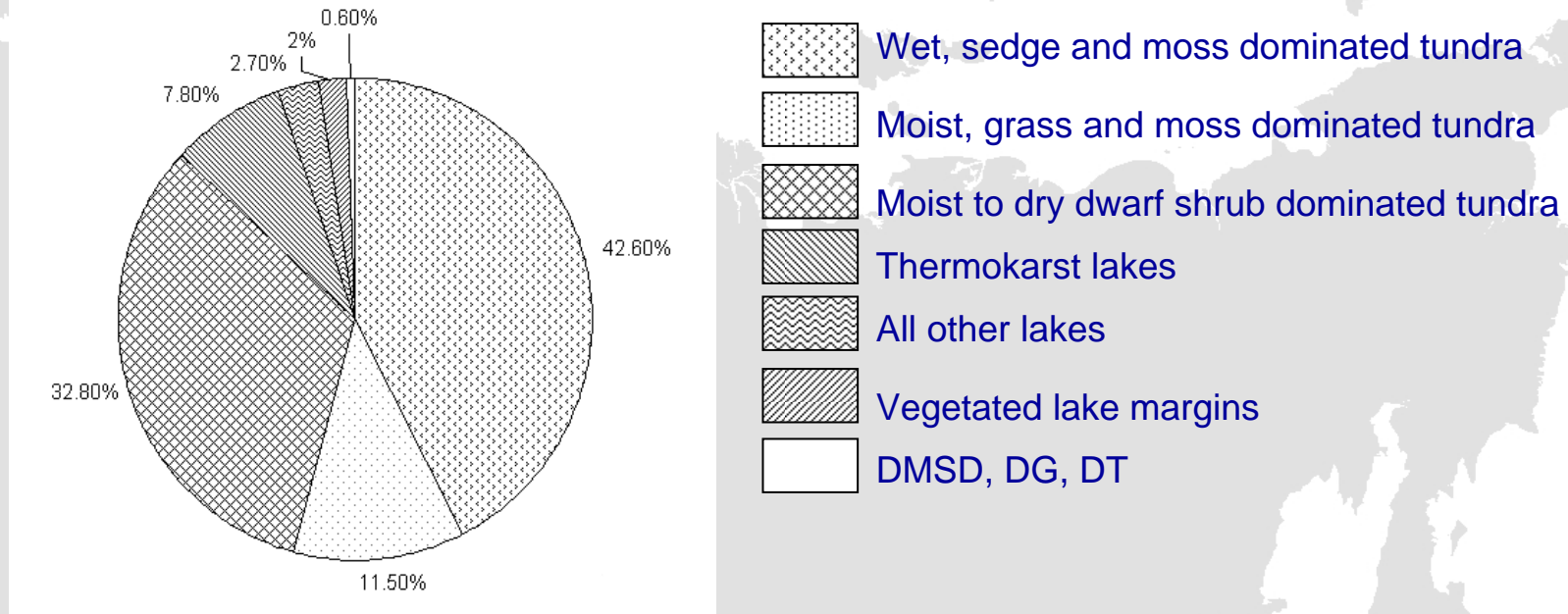
J. Schneider, G. Grosse, D. Wagner



- mainly non-vegetated areas;
- dry to moist, dwarf shrub dominated tundra
- dry grass and dwarf shrub dominated tundra
- dry sandy, moss, sedge, and dwarf shrub dominated tundra
- wet sedge and moss dominated tundra
- moist sedge and moss dominated tundra

Methane Fluxes from Periglacial Landscapes in the Lena River Delta

J. Schneider, G. Grosse, D. Wagner



Percentage of methane emissions of individual land cover classes based on the total methane emission of the Lena Delta.

Total delta area:

29 036 km²

Mean daily methane emission (July):

10.35 mg CH₄ m⁻²d⁻¹.

Annual methane emission:

972 mg m⁻² a⁻¹ or ~0.03 Tg

Spectral Properties of Periglacial Landscapes in the Lena Delta

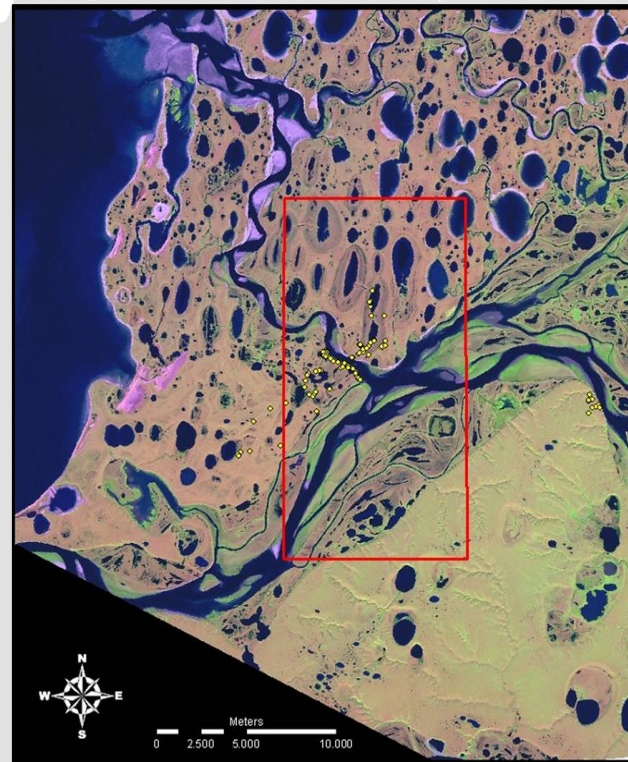
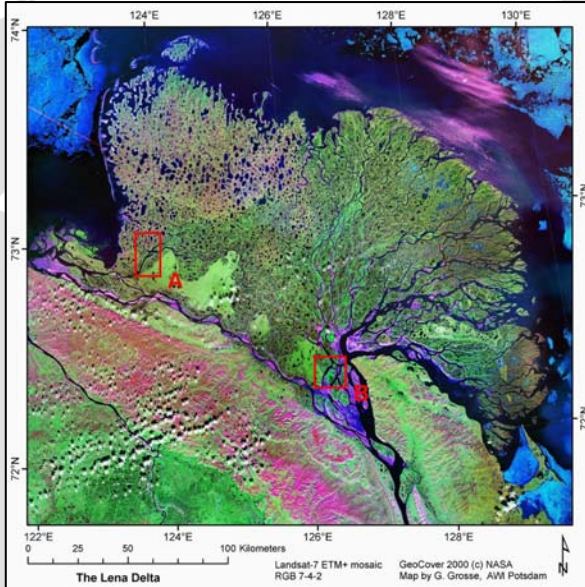
M. Ulrich, G. Grosse, L. Schirrmeister

Objectives

- Characterization and classification of typical periglacial surfaces
- Development of a spectral database for periglacial / tundra surfaces

Study area

- Covers all 3 main terraces of the Lena Delta
- Contains a wide range of periglacial surface features



Spectral Properties of Periglacial Landscapes in the Lena Delta

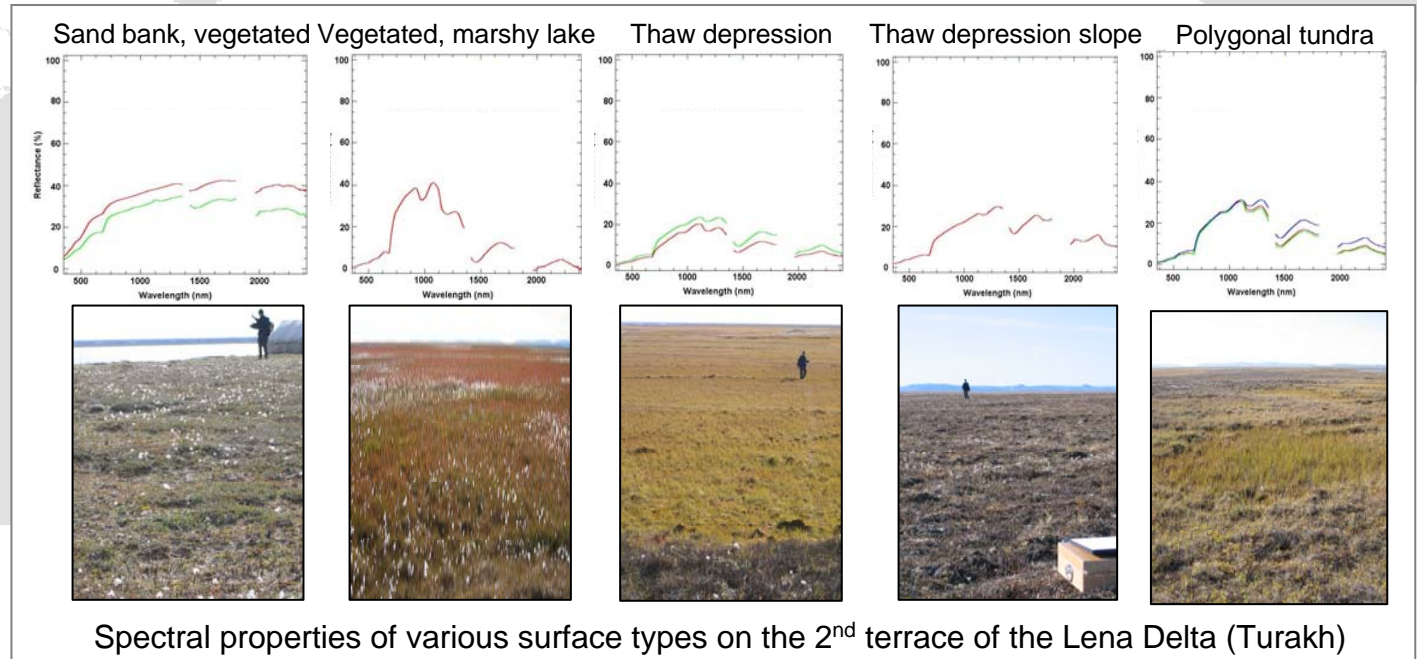
M. Ulrich, G. Grosse, L. Schirrmeister

	LANDSAT 7 ETM+	CHRIS/PROBA Mode 3 Land Channels	ASD FieldSpec-FR™
Sensor height	705 km	556 km	~1 m
Coverage	185 km swath width	13 x 13 km	Points
Spatial resolution	30 x 30 m (VIS-SWIR) 15 x 15 m (pan) 120 x 120 m (TIR)	17 x 17 m (VIS-VNIR)	ca. 0,4 x 0,4 m (VIS-SWIR) (when instrument height above target is 1m and 24° fore optics used)
Spectral bands	8 for 450-12500 nm	18 for 438 – 1035 nm	512 for 350 – 1000 nm 1060 for 1000 – 2500 nm 2151 interpolated for every nanometer
Wavelengths	450 – 520 nm 530 – 610 nm 620 – 690 nm 780 – 900 nm 1550 – 1750 nm 10400 – 12500 nm 2090 – 2350 nm 520 – 900 nm (pan)	438 – 447 nm, 486 – 495 nm 526 – 534 nm, 546 – 556 nm 566 – 573 nm, 627 – 636 nm 656 – 666 nm, 666 – 677 nm 694 – 700 nm, 700 – 706 nm 706 – 712 nm, 738 – 745 nm 745 – 752 nm, 773 – 788 nm 863 – 881 nm, 891 – 900 nm 900 – 910 nm, 1002 – 1035 nm	Band width 3 nm for 350 – 1000 nm 10 nm for 1000 – 2500 nm

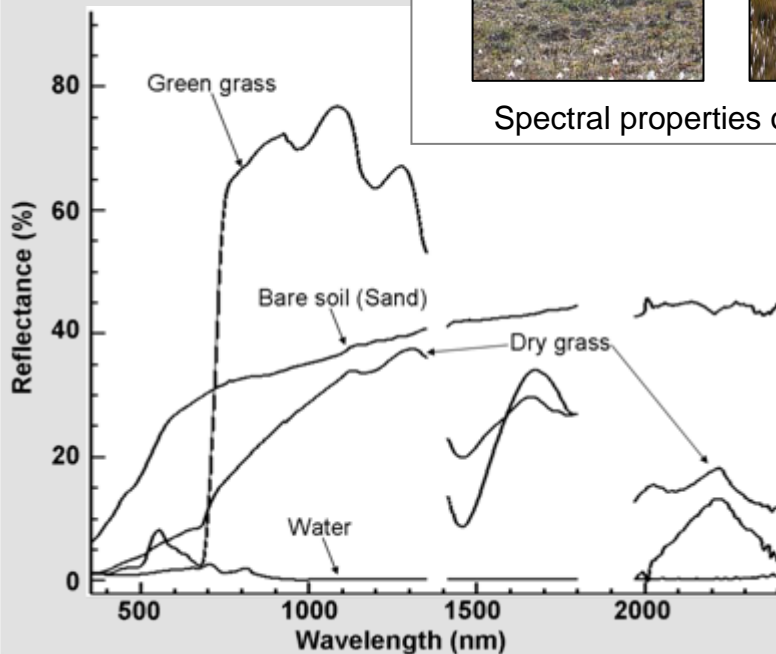


Spectral Properties of Periglacial Landscapes in the Lena Delta

M. Ulrich, G. Grosse, L. Schirrmeister



Spectral properties of various surface types on the 2nd terrace of the Lena Delta (Turakh)



Results

- 12 spectral classes derived from field spectral measurements
- periglacial surfaces can be well distinguished by their spectral properties

Spectral signatures of green and dry grass, bare soil and water in tundra landscapes (August 2005) using an ASD FieldSpec Pro FR®. Atmospheric water absorption bands around 1400 nm and 1900 nm are masked.

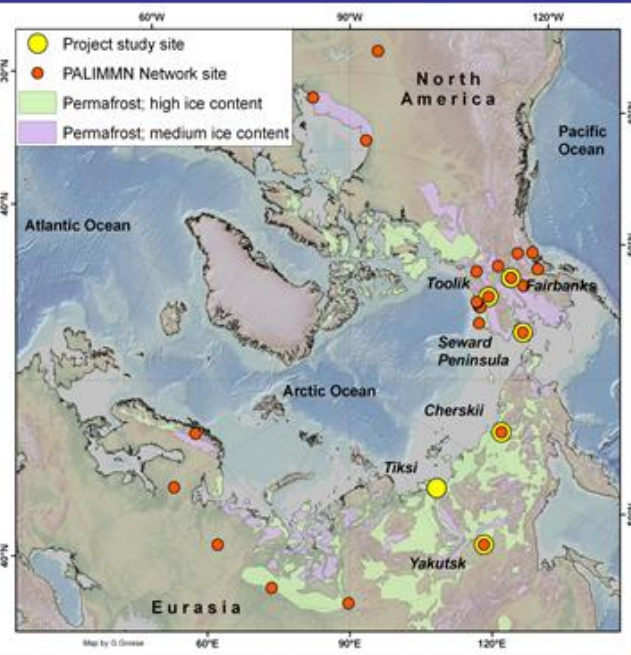
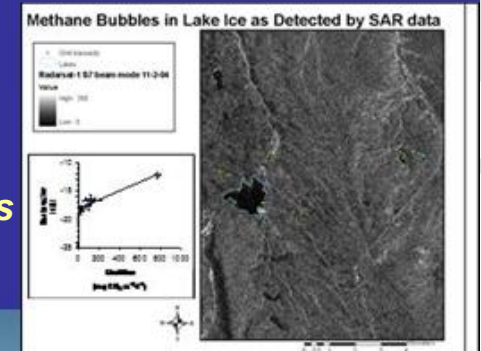


Upcoming projects

Pan-Arctic Lake-Ice Methane Monitoring Network

PALIMMN

K. Walter, G. Grosse *et al.*
University of Alaska, Fairbanks



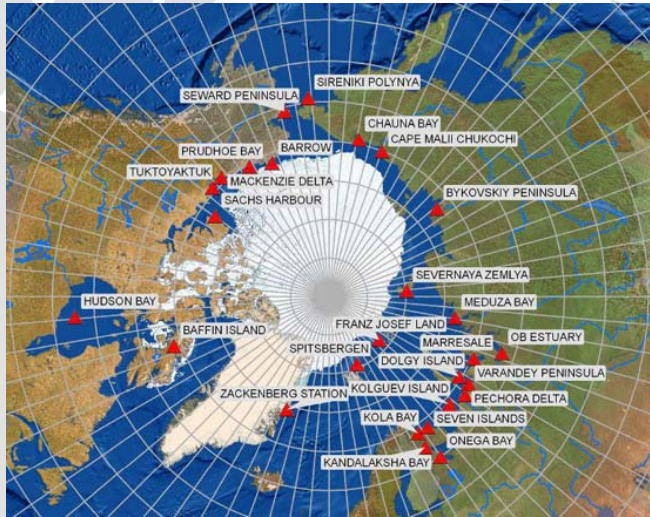
NSF Arctic Observing Network



'An open network to quantify methane emissions from northern lakes'

Remote Sensing Baseline for Long-Term Monitoring of the Arctic Circumpolar Coastal Observatory Network (ACCO-Net)

P. Overduin, H. Lantuit, M. Allard, G. Grosse, & the ACCO-Net Steering Committee



- 2007-2009

- Aims at the acquisition and analysis of multi-sensoral + multi-temporal remote sensing data for the ACCO-Net project (IPY Activity ID: 90) and its sites (currently 41)

- Imagery sponsored by ESA IPY programme:

--> new ALOS PRISM + AVNIR-2 images

--> archived + new SPOT images

Goal of this project is to deliver important base data for the ACCO-Net objectives

- establish the rates and magnitudes of erosion and accumulation of Arctic coasts;
- estimate the amount of sediments and organic carbon derived from coastal erosion;
- refine and apply an Arctic coastal classification (incl. ground ice, permafrost, geology, etc.);
- produce a series of thematic and derived maps (e.g. coastal classification, ground-ice, sensitivity etc.);



Thank you!

Collaborators:

Vladimir Romanovsky, GI UAF

Katey Walter, INE / IARC UAF

Hugues Lantuit, AWI for Polar and Marine Research Potsdam, Germany

Anne Morgenstern, AWI for Polar and Marine Research Potsdam, Germany

Lutz Schirrmeister, AWI for Polar and Marine Research Potsdam, Germany

Paul Overduin, AWI for Polar and Marine Research Potsdam, Germany

Julia Schneider, University of Greifswald, Institute of Botany and Landscape Ecology

Mathias Ulrich, University of Leipzig, Department of Geography, Germany

+ several other colleagues from Alaska, Russia, and Germany